

AD-A074 366

NAVAL SURFACE WEAPONS CENTER DAHLGREN LAB VA
CAPACITOR GAUGE FOR GAS GUN EXPERIMENTS.(U)
JUN 79 E J SHULER, W MOCK, W H HOLT
NSWC/TR-79-192

F/G 14/2

UNCLASSIFIED

NL

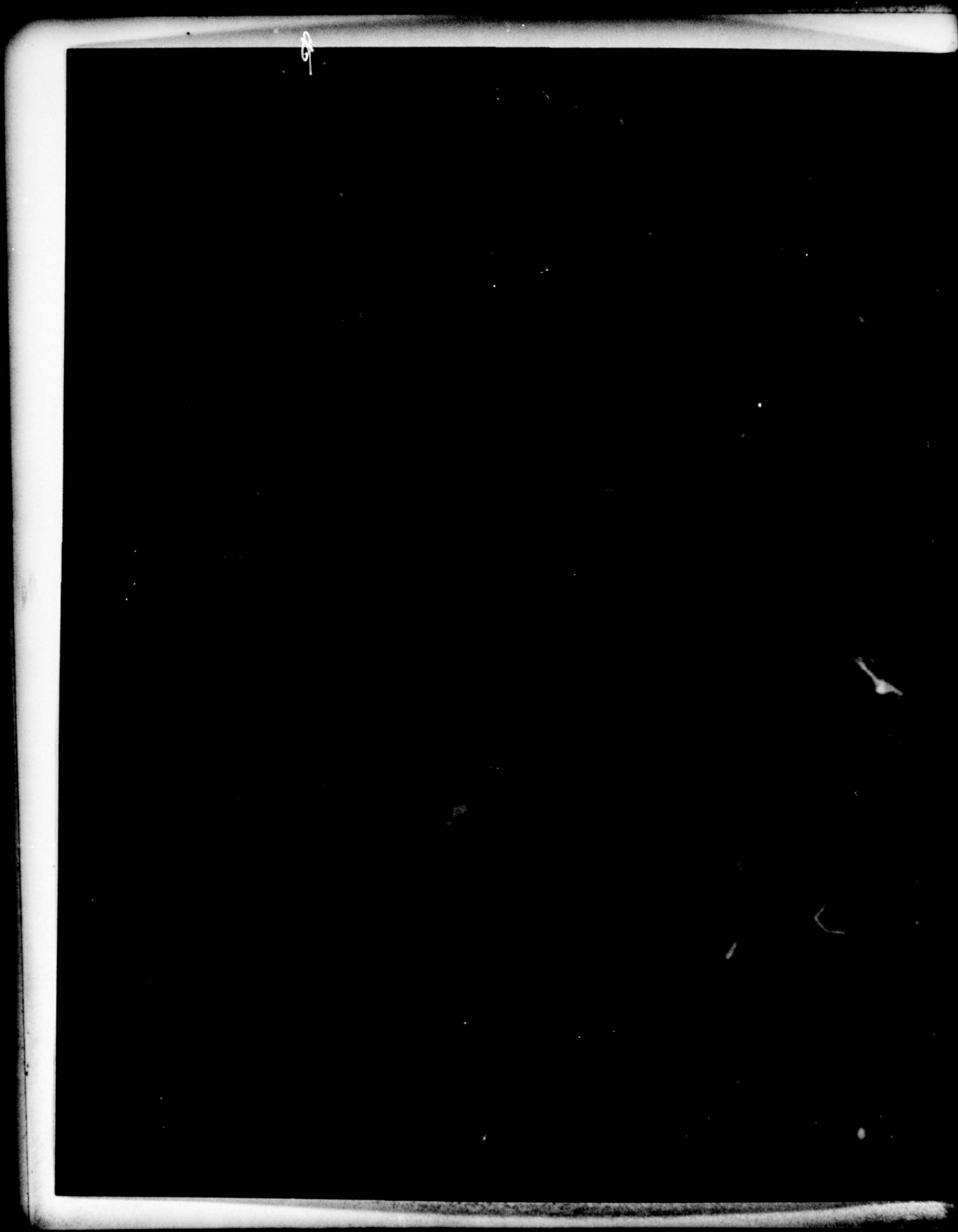
1 OF 1
AD
A074366



DA074366

12 LEVEL II

DDC
RECEIVED
SEP 27 1979
B



REPORT DOCUMENTATION PAGE		READ INSTRUCTIONS BEFORE COMPLETING FORM
1. REPORT NUMBER 14 NSWC/TR-79-192	2. GOVT ACCESSION NO.	3. RECIPIENT'S CATALOG NUMBER
4. TITLE (and Subtitle) 6 CAPACITOR GAUGE FOR GAS GUN EXPERIMENTS	5. TYPE OF REPORT & PERIOD COVERED 9 Final rept.	6. PERFORMING ORG. REPORT NUMBER
7. AUTHOR(s) 10 E. J. Shuler, W. Mock, Jr., W. H. Holt	8. CONTRACT OR GRANT NUMBER(s) 12 53	10. PROGRAM ELEMENT, PROJECT, TASK AREA & WORK UNIT NUMBERS SF-33-354-391 SF-32-392-391
9. PERFORMING ORGANIZATION NAME AND ADDRESS Naval Surface Weapons Center (G30) Dahlgren, Virginia 22448	11. CONTROLLING OFFICE NAME AND ADDRESS Naval Sea Systems Command Washington, D. C. 20362	12. REPORT DATE 11 June 1979
14. MONITORING AGENCY NAME & ADDRESS (if different from Controlling Office) 16 F33354, F32392 17 SF 33354 391, SF32392 391	13. NUMBER OF PAGES 55	15. SECURITY CLASS. (of this report) UNCLASSIFIED
16. DISTRIBUTION STATEMENT (of this Report) Approved for public release; distribution unlimited. 62633		15a. DECLASSIFICATION/DOWNGRADING SCHEDULE
17. DISTRIBUTION STATEMENT (of the abstract entered in Block 20, if different from Report)		
18. SUPPLEMENTARY NOTES		
19. KEY WORDS (Continue on reverse side if necessary and identify by block number) Capacitor gauge Instrumentation Shock waves Impact Gas gun		
20. ABSTRACT (Continue on reverse side if necessary and identify by block number) → This report describes the fabrication, calibration, and operation of a capacitor gauge that has been designed for use with the NSWC gas gun. The gauge was adapted from a Lawrence Livermore Laboratory capacitor gauge. A capacitor gauge measures the shock-induced motion of the free surface of a material specimen. The read time for the gauge is about 1 ms ^{microsec} when used with this gas gun. ←		

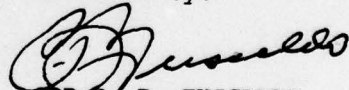
DDC
RECEIVED
SEP 27 1979
B

FOREWORD

This report describes a capacitor gauge that has been designed for use with the NSWC gas gun. It is used for measuring mechanical shock properties of materials. This work was supported by NAVSEA Block Nos. SF-33-354-391 and SF-32-392-391.

This report has been reviewed by Hugh E. Montgomery, Head, Technology Branch; and C. L. Dettinger, Acting Head, Gun Systems and Munitions Division.

Released by:



CDR R. P. FUSCALDO
Assistant for Weapons Systems
Weapons Systems Department

PRECEDING PAGE BLANK

ACCESSION for		
NTIS	White Section	<input checked="" type="checkbox"/>
DDC	Buff Section	<input type="checkbox"/>
UNANNOUNCED		<input type="checkbox"/>
JUSTIFICATION _____		
BY _____		
DISTRIBUTION/AVAILABILITY CODES		
Dist.	AVAIL.	and/or SPECIAL
A		

ACKNOWLEDGEMENT

The authors would like to acknowledge J. W. Forbes for helpful discussions. They would also like to acknowledge D. L. Banner and A. Romero of Lawrence Livermore Laboratory for helpful discussions and for providing engineering drawings for a capacitor gauge and a computer program for data reduction.

CONTENTS

	<u>Page</u>
FOREWORD	iii
ACKNOWLEDGEMENT	v
LIST OF ILLUSTRATIONS	ix
LIST OF TABLES	x
EXECUTIVE SUMMARY	xi
I. INTRODUCTION	1
II. FABRICATION AND CALIBRATION OF CAPACITOR GAUGE	3
III. OPERATION OF CAPACITOR GAUGE	13
REFERENCES	18
APPENDIXES	
A--ENGINEERING DRAWINGS FOR CAPACITOR GAUGE	19
B--PLOTS FOR DETERMINING CAPACITOR GAUGE SPACER THICKNESSES AND OSCILLOSCOPE SETTINGS FOR VARIOUS FREE-SURFACE-VELOCITY VALUES	31
C--INTEGRATION OF CAPACITOR GAUGE VOLTAGE PULSE USING THE TRAPEZOIDAL AND SIMPSON'S RULES	41
DISTRIBUTION	

LIST OF ILLUSTRATIONS

<u>Figure</u>		<u>Page</u>
1	Schematic of gas gun.	1
2	Schematic of muzzle region showing a target assembly with a capacitor gauge.	2
3	Calibration of capacitor gauge.	5
4	Capacitor gauge calibration curve	7
5	Schematic of capacitor gauge and voltage-limiter circuits. . . .	8
6	Completed capacitor gauge.	9
7	Completed target assembly with a capacitor gauge.	12
8	Oscilloscope data from target assembly with a capacitor gauge. .	15
9	Free-surface velocity versus time profile for 6061-T6 aluminum. .	16
A-1	Capacitor gauge assembly.	21
A-2	Capacitor gauge spacer.	22
A-3	Capacitor gauge body.	23
A-4	Capacitor gauge insulator.	24
A-5	Capacitor gauge flange.	25
A-6	Capacitor gauge center conductor 1.	26
A-7	Capacitor gauge center conductor 2.	27
A-8	Capacitor gauge case.	28
A-9	Capacitor gauge end cap.	29
B-1	Capacitor gauge voltage-time profiles for 6.4- and 10.2-mm-diameter gauge disks and selected spacer thicknesses at a constant specimen free-surface velocity of 0.1 km/s.	35
B-2	Capacitor gauge voltage-time profiles for 6.4- and 10.2-mm-diameter gauge disks and selected spacer thicknesses at a constant specimen free-surface velocity of 0.5 km/s.	36

LIST OF ILLUSTRATIONS (Continued)

<u>Figure</u>		<u>Page</u>
B-3	Capacitor gauge voltage-time profiles for 6.4- and 10.2-mm-diameter gauge disks and selected spacer thicknesses at a constant specimen free-surface velocity of 1 km/s.	37
B-4	Initial capacitor gauge voltage versus specimen free-surface-velocity curves for selected spacer thicknesses for a 6.4-mm-diameter gauge disk.	38
B-5	Initial capacitor gauge voltage versus specimen free-surface-velocity curves for selected spacer thicknesses for a 10.2-mm-diameter gauge disk.	39
B-6	Normalized time to attain final capacitor gauge voltage versus specimen free-surface velocity for selected spacer thicknesses.	40
C-1	Free-surface velocity versus time profile for 6061-T6 aluminum using the trapezoidal and Simpson's rules for integration of the capacitor gauge voltage-time pulse.	45

LIST OF TABLES

<u>Table</u>		<u>Page</u>
1	Measurement of gauge capacitance versus specimen spacing.	6
2	Digitized capacitor gauge voltage data and the corresponding free-surface-velocity and free-surface-position results for 6061-T6 aluminum.	14
3	Summary of shock-wave results for 6061-T6 aluminum.	17
C-1	Free-surface-velocity and free-surface-position results using the trapezoidal and Simpson's rules for integrating the capacitor gauge voltage pulse.	44

EXECUTIVE SUMMARY

A capacitor gauge for performing real-time shock-wave measurements in materials is described. The gauge was designed for use with the NSW 40-mm-bore gas gun and was adapted from a Lawrence Livermore Laboratory capacitor gauge. One plate of the capacitor is the material specimen to be impacted. The shock-generated free-surface motion of the impacted specimen is measured with the gauge. This report describes in detail the fabrication and calibration procedures for the capacitor gauge. The capacitor gauge engineering drawings are included in the report. A description of the operation of the capacitor gauge and the data analysis procedures are presented. Plots are presented to simplify the oscilloscope adjustment for a capacitor gauge experiment. An impact experiment with 6061-T6 aluminum was performed to check the operation of the gauge; the results are in good agreement with previous experiments.

I. INTRODUCTION

This report describes a capacitor gauge that has been designed for use with the NSWG gas gun.¹ The gauge was adapted from a Lawrence Livermore Laboratory capacitor gauge.² The capacitor gauge technique described here is originally due to Rice. A capacitor gauge is used for determining the shock properties of materials.²⁻⁴ The free surface of the material specimen to be studied forms one plate of a parallel plate capacitor (for a conducting specimen a thin metallic film may be deposited on the free surface). The gauge measures the shock-generated free-surface motion of the specimen. The shock wave could be produced by projectile impact or explosive detonation, or by other means.

In this report a 40-mm-bore gas gun is used for generating the shock waves in the specimen. A schematic of the gas gun is shown in Figure 1. A projectile with an impactor disk is loaded into the barrel, and a target assembly containing the specimen and a capacitor gauge is mounted on the muzzle of the gun. The barrel is evacuated to 0.1 Pa pressure to minimize gas cushion effects at impact. The gun is fired by actuating the fast-opening valve. The projectile impact velocity can be varied in a controlled manner over the range from 0.03 to 1 km/s.

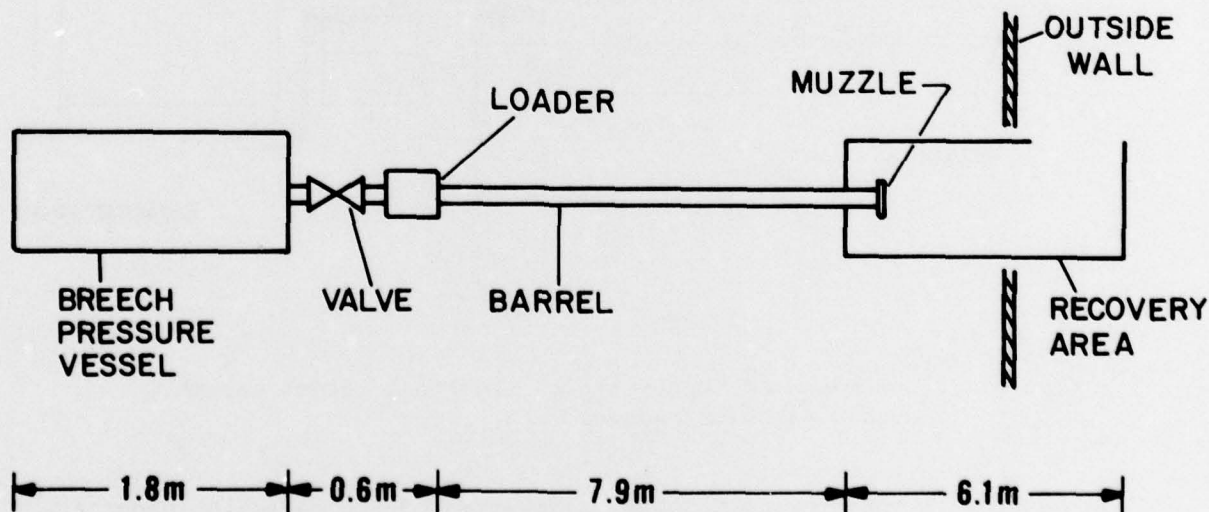


Figure 1. Schematic of gas gun.

Figure 2 is a schematic of the muzzle region for a target assembly containing a capacitor gauge. The average projectile velocity at impact is measured with the three charged pins in the side of the barrel. The time of impact is measured with four charged tilt pins which are placed around the specimen. The tilt pin ends are positioned in the plane of the impact face of the specimen to within $1\text{ }\mu\text{m}$. The capacitor gauge is spaced a preselected distance behind the specimen and measures the shock-induced free-surface motion of the back face of the specimen. The shock transit time is determined by measuring the time difference between the tilt output signal and the capacitor gauge signal.

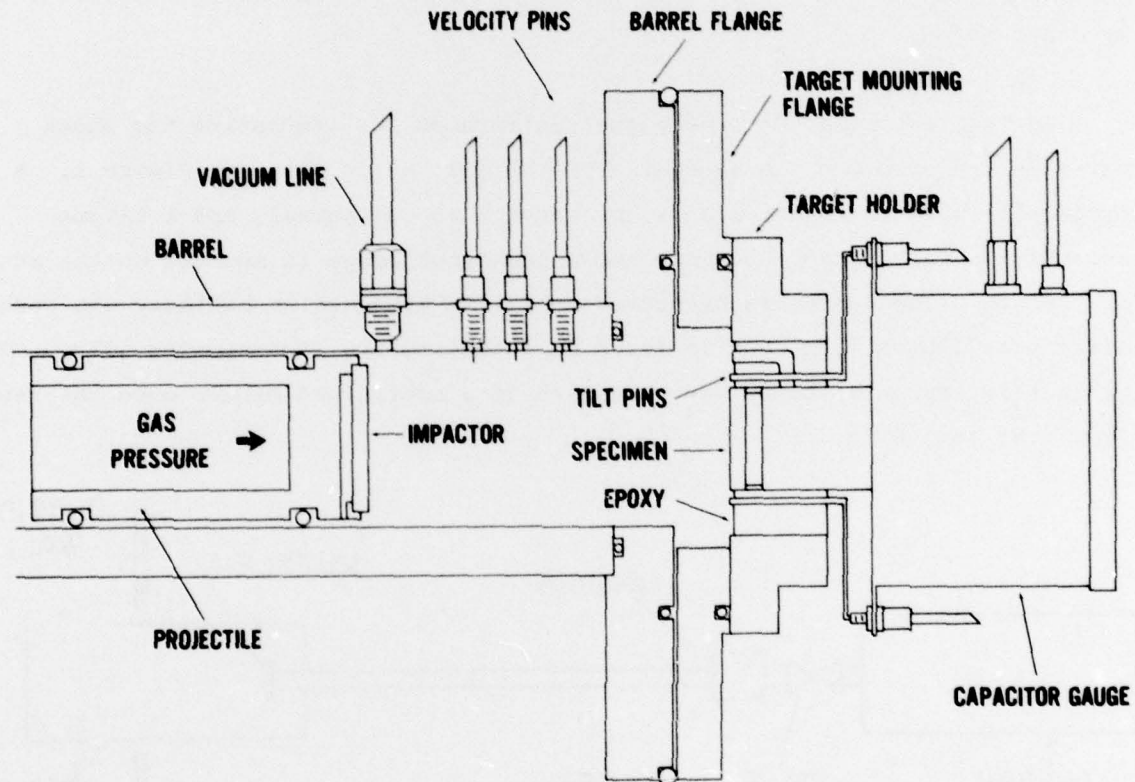


Figure 2. Schematic of muzzle region showing a target assembly with a capacitor gauge.

In Section II the fabrication and calibration of the capacitor gauge are discussed. The operation of the gauge is presented in Section III. Appendix A

contains the engineering drawings for the NSWC capacitor gauge. Appendix B contains plots for determining the spacer thickness and oscilloscope settings for a capacitor gauge as a function of the specimen free-surface velocity. Appendix C contains the results of integrating the capacitor gauge voltage-time pulse using the trapezoidal and Simpson's rules.

II. FABRICATION AND CALIBRATION OF CAPACITOR GAUGE

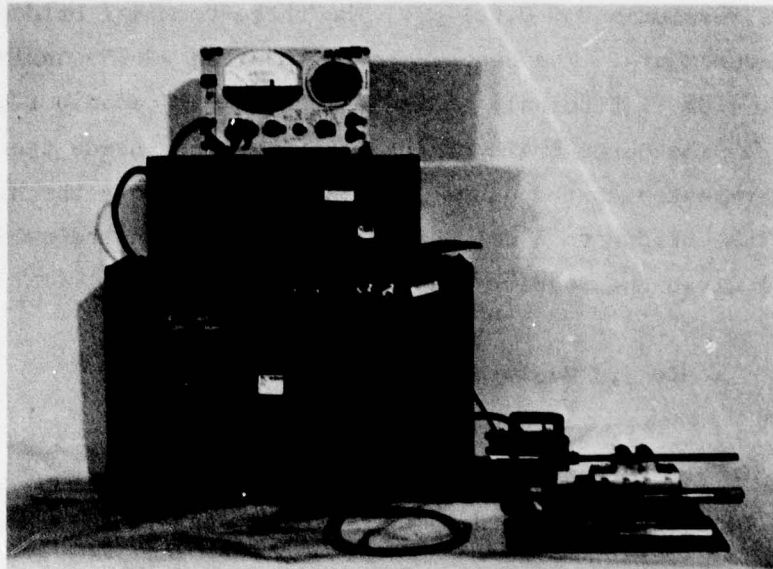
The first step in the fabrication procedure consists of soldering the case and flange pieces of the capacitor gauge together (see Appendix A). Next, a copper tube (3.17-mm outside diameter, 0.64-mm wall thickness, and approximately 37-mm long) is soldered into the 3.45-mm-diameter hole in the body piece. Low-temperature silver solder is used for these soldering operations. The copper tube allows the capacitor gauge region behind the specimen to be evacuated along with the gun barrel. A vacuum reduces the possibility of electrical breakdown between the high-voltage center conductor and the grounded gauge body and specimen. It also eliminates the possibility that the capacitor gauge signal will be affected by air compression in the region behind the specimen.

The next step in the fabrication procedure is to attach the brass center conductor to the gauge body. Center conductor 1 (see Figure A-6) having a disk diameter of 10.16 mm was selected for this gauge. Nylon screws are placed in the three 2-56 UNC holes in the brass body until they are flush with the inside wall of the body. The body, center conductor, and a Lucite insulator are then assembled and aligned on a flat granite surface plate. The faces of the center conductor disk and body are therefore assured of being in the same plane. Alumina-filled epoxy (Castall 300-RT 7) is then poured into the recessed regions of the body and insulator until the epoxy is flush with the top of the body (see Figure A-1). The close tolerances of the three pieces ensure that no epoxy seeps into the cavity region of the center conductor-body assembly. After the epoxy cures, the nylon screws are removed from the body. The face of the center conductor-body assembly is then lapped flat with #2/0 and #4/0 Buehler emery paper on a granite surface plate. The flange-case

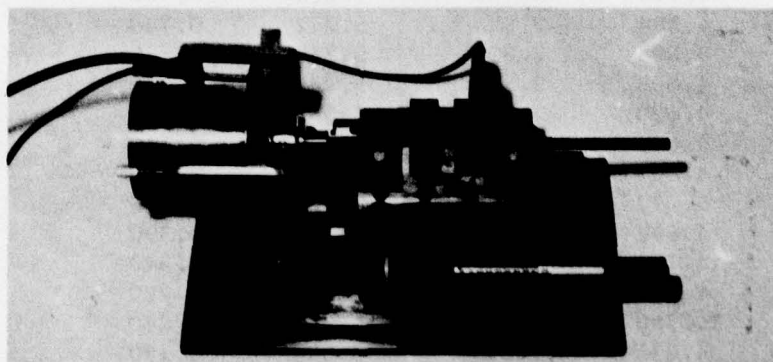
assembly is then attached to the center conductor-body assembly with three 2-56 UNC brass screws. The gauge is now ready for calibration.

The purpose of the calibration procedure is to measure the small capacitance between the center conductor and a simulated specimen face as the spacing between the specimen and center conductor is varied. The body, flange, case, and end cap of the gauge introduce a constant shunt capacitance which is included in the measurement. (A brass end cap is attached to the gauge for the calibration procedure.)

Figure 3(a) shows the experimental setup for calibrating the capacitor gauge. A capacitance bridge system (General Radio Company) was used for the measurements. The electronic items consist of a null indicator (Model 1232-A) and high-input impedance preamplifier (Model 1232-P2) shown at the top, a regulated power supply (Model 1201-B), an oscillator (Model 1210-C) shown in the middle, and a capacitance bridge (Model 1615-A) shown at the bottom. The mechanical calibration device with the attached capacitor gauge is shown to the right of the electronic items in Figure 3(a). The calibration device is the same device^{1,5} that is used for measuring the spacing of the velocity pins (see Figure 2). Figure 3(b) is a close-up view of the calibration device and the attached capacitor gauge. A 28-mm-diameter disk simulates the target specimen. The gauge is attached to the vertical flange of the calibration device with two small C-clamps. Metal shim stock is used to ensure that the gauge and specimen faces are in approximate parallel planes. The calibration device micrometer has a resolution of 0.002 mm. The maximum specimen position x_0 is obtained by placing a 3.19-mm-thick brass spacer between the gauge and specimen faces. (This is the same spacer that is used in the target assembly.) The uncertainty in this spacing measurement is about 0.01 mm and is due to the slight nonparallelism of the gauge and specimen planes. The gauge capacitance is measured for this maximum spacing.



(a)



(b)

Figure 3. Calibration of capacitor gauge. (a) Overall view showing calibration device and electronic equipment. (b) Close-up view showing capacitor gauge attached to calibration device.

The spacer is then removed and capacitance measurements are made as the specimen spacing is decreased. The measurements are made at a frequency of 1 kHz and have a resolution of 0.001 pF. The three-terminal bridge mode is used for the measurements. The center conductor of an RG-55 coaxial cable connects the low side (L terminal) of the bridge to the capacitor gauge center conductor. The outer braid of the cable extends inside the gauge case and is unterminated at the gauge. A clip lead connects the high side (H terminal) of the bridge to a convenient ground point on the calibration device. Table 1 gives the results of the measurements.

Table 1. Measurement of gauge capacitance versus specimen spacing.^a

Gauge Capacitance (pF)	Specimen Spacing (mm)	Gauge Capacitance (pF)	Specimen Spacing (mm)
4.521	3.190	4.906	1.140
4.527	3.090	4.936	1.090
4.534	2.990	4.969	1.040
4.540	2.890	5.007	0.990
4.547	2.790	5.047	0.940
4.555	2.690	5.094	0.890
4.564	2.590	5.145	0.840
4.574	2.490	5.204	0.790
4.584	2.390	5.272	0.740
4.595	2.290	5.349	0.690
4.608	2.190	5.440	0.640
4.623	2.090	5.547	0.590
4.639	1.990	5.676	0.540
4.657	1.890	5.829	0.490
4.677	1.790	6.020	0.440
4.699	1.690	6.264	0.390
4.726	1.590	6.580	0.340
4.756	1.490	7.022	0.290
4.790	1.390	7.656	0.240
4.831	1.290	8.638	0.190
4.879	1.190	10.47	0.140

^aThese calibration measurements were made using the test setup shown in Figure 3.

Figure 4 is a plot of the measured gauge capacitance versus inverse specimen spacing. The curve shown in the figure was obtained by fitting to the initial 16 data points. First a curve of the form $C = Ax^{-1} + B$ is fitted to the data points using the method of least squares. This gives values for the parameters A and B. For this gauge $A = 0.6390$ pF mm and $B = 4.318$ pF. B represents the small constant shunt capacitance of the gauge disk. Then a curve of the form

$$C = \frac{A}{x - D} + B, \quad (1)$$

is fitted to the same data points to obtain a value for the parameter D. This parameter is used to account for the nonlinearity in the data points as x^{-1} increases. The nonlinearity may be due to the measurement uncertainty in determining the initial specimen spacing and capacitive edge effects. D is obtained by trial and error to the nearest 0.001 mm by selecting the value that gives the minimum deviation between the computed and experimental capacitance values. The deviation was taken as $P = N^{-1} \left[\sum_{i=1}^N (C(x_i) - C_i(x_i))^2 \right]^{1/2}$

where $N = 16$, and $C(x_i)$ and $C_i(x_i)$ are the computed and experimental capacitance values, respectively, at the measured spacing x_i . For this gauge $D = 0.047$ mm.

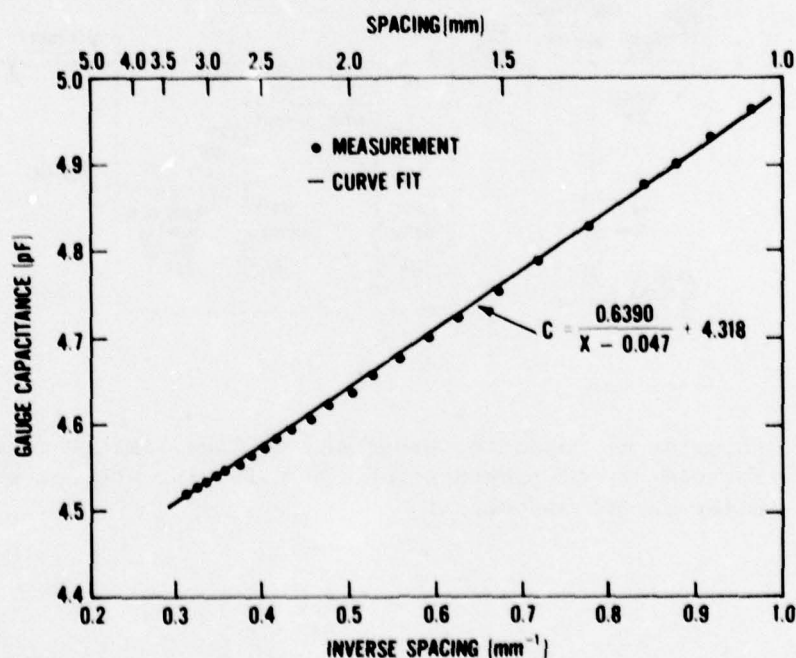


Figure 4. Capacitor gauge calibration curve. The points represent the initial 24 measurements from Table 1. Also shown is the best-fit curve using the initial 16 points; C is the gauge capacitance and x is the spacing.

The next step in the fabrication procedure consists of completing the electrical circuit for the capacitor gauge. Figure 5 is the electrical schematic of the capacitor gauge and the voltage-limiter circuits. The gauge disk and the 0.01- μ F coupling capacitor are charged to a voltage of -3 kV, the latter being charged through the 50- Ω termination at the oscilloscope. The charging supply is isolated from the gauge circuit with the 1.5-M Ω resistor. At projectile impact the specimen disk moves toward the right and increases the gauge capacitance. Charge flows onto the gauge to maintain the voltage at -3 kV. The flowing charge produces a voltage across the 50- Ω termination resistance which is recorded on the oscilloscope. The purpose of the voltage-limiter circuit is to protect the oscilloscope from voltage overload as the measured voltage increases. This circuit is isolated from the gauge circuit until a clipping voltage of about ± 12 V is approached. Figure 6 is a view of the completed capacitor gauge showing the electrical components inside the gauge and the gauge disk and spacer.

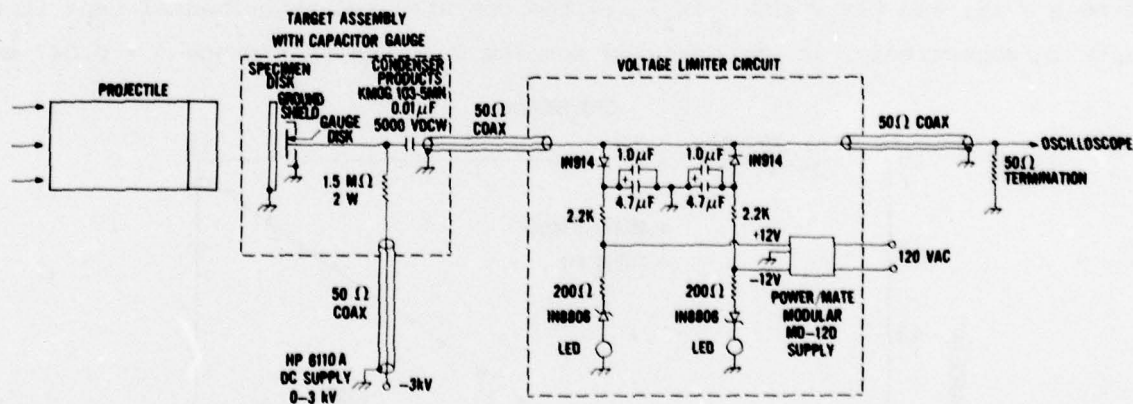
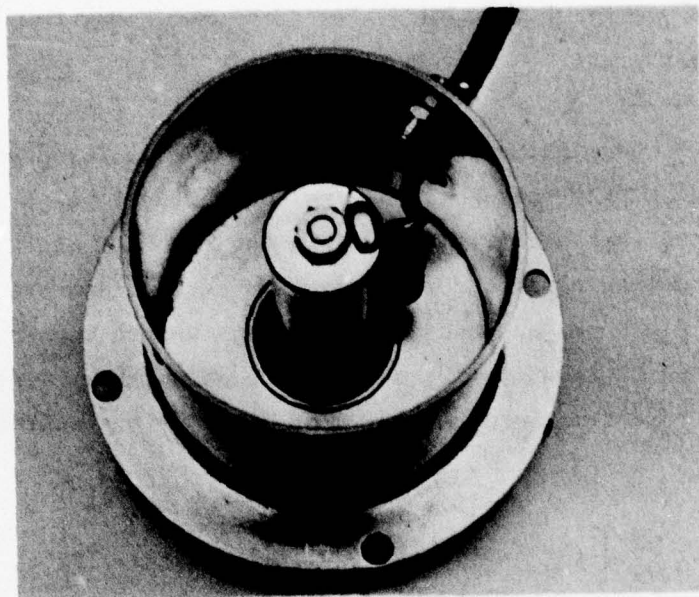
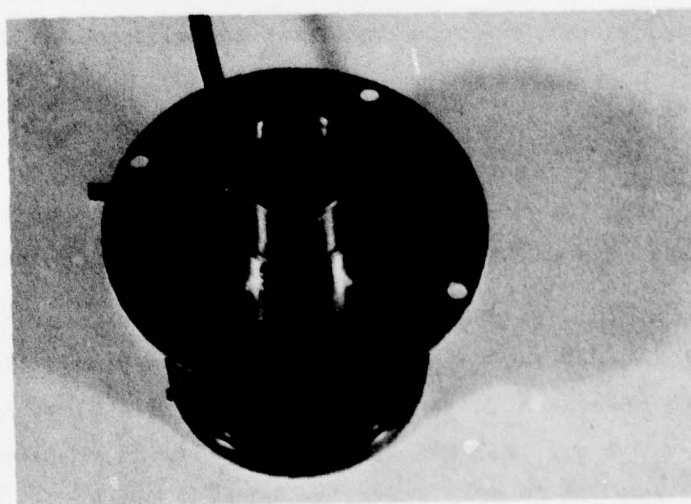


Figure 5. Schematic of capacitor gauge and voltage limiter circuits. (For clarity of presentation the tilt pins are not shown in the target assembly.)



(a)



(b)

Figure 6. Completed capacitor gauge. (a) View of gauge with end cap removed showing the $0.01\text{-}\mu\text{F}$ coupling capacitor and the $1.5\text{-M}\Omega$ resistor inside the brass case. (b) View of gauge showing the flange, spacer, and center conductor.

Following Rice² the equation describing the circuit in Figure 5 is given by

$$RC \frac{dV}{dt} + V = -RE_0 \frac{dC}{dt}, \quad (2)$$

where R is the 50- Ω termination resistance, V is the measured voltage across R, E_0 is the -3 kV dc supply voltage, and C is the measured gauge capacitance. The two assumptions that were made to obtain Equation (2) are $C_0 \gg C$ and $E_0 \gg V$. Here C_0 is the coupling capacitance. These two assumptions are satisfied since $C_0 = 0.01 \mu F$ and $C \approx 5 pF$, and the output voltage V is always much less than E_0 . Following Reference 2, Equation (2) can be reduced further. Integrating this equation over a short-time interval in which C and $\frac{dC}{dt}$ are approximated as constants gives

$$V = -RE_0 \frac{dC}{dt} \left[1 - \exp\left(-\frac{t}{RC}\right) \right], \quad (3)$$

where $V(0) = 0$. The time constant is $RC \approx 0.25 ns$. ($RC \approx 30 ns$ for Rice's circuit.²) Thus after a few time constants (which is much shorter than the typical microsecond read time for a capacitor gauge) Equation (3) can be approximated with

$$V = -RE_0 \frac{dC}{dt}. \quad (4)$$

Using this equation is equivalent to assuming that $V \gg RC \frac{dV}{dt}$ in Equation (2).

A test shot was performed to check the operation of the capacitor gauge. For this shot the initial fast-rising plastic wave portion of the voltage pulse (the pulse will be presented in the next section) has a slope of $\frac{dV}{dt} \approx 0.5 mV ns^{-1}$ and a voltage of $V \approx 7 mV$. For the later slower-rising portion of this pulse $\frac{dV}{dt} \approx 0.01 mV ns^{-1}$ and $V \approx 10 mV$. Therefore $RC \frac{dV}{dt} \approx 0.1$ and $0.003 mV$ for the fast- and slow-rising portions of the pulse, respectively. These values are about 2 and 0.003% of the voltages in the two regions, respectively. These results show that negligible error will be introduced by using Equation (4).

The specimen free-surface velocity U_{fs} can be obtained from the equation

$$U_{fs} = - \frac{dx}{dt} = - \left(\frac{dC}{dt} \right) / \left(\frac{dC}{dx} \right). \quad (5)$$

Here $\frac{dC}{dt}$ is obtained from the measured voltage-time profile (Equation (4)), and $\frac{dC}{dx}$ is obtained by differentiating the measured capacitor gauge calibration curve (Equation (1)). Making these substitutions into Equation (5) gives

$$U_{fs} = - \frac{V}{RE_0 A} (x - D)^2 . \quad (6)$$

It is possible to eliminate the specimen free-surface position x from Equation (6). First, Equation (4) is integrated to obtain

$$C - C_0 = - \frac{1}{RE_0} \int_0^t v \, dt , \quad (7)$$

where x_0 is the initial specimen spacing and $C_0 = C(x_0)$. Substituting for C and C_0 from Equation (1) gives

$$x(t) = D + \frac{x_0 - D}{1 - \frac{(x_0 - D)}{RE_0 A} \int_0^t v \, dt} . \quad (8)$$

Substituting Equation (8) into Equation (6) finally gives for the free-surface velocity

$$U_{fs} = - \frac{(x_0 - D)^2}{RE_0 A} \frac{V}{\left[1 - \frac{(x_0 - D)}{RE_0 A} \int_0^t v \, dt \right]^2} . \quad (9)$$

Equations (8) and (9) are used in the next section to obtain the specimen free-surface position and velocity at selected times from the measured voltage-time pulse.

A target assembly with a 6061-T6 aluminum specimen was prepared to check the operation of the capacitor gauge. Standard target preparation techniques were used to prepare the target assembly with the aluminum specimen and four tilt pins.¹ The tilt pins are fabricated from 0-80 stainless steel threaded rod. A hole is drilled in the epoxy material of the target assembly to accept

the copper vacuum tube that is located in the side of the capacitor gauge. The vacuum tube is then bent perpendicular to the face of the gauge and cut to an appropriate length so that it will be recessed from the impact face of the specimen when the gauge and a spacer are placed on the back face (opposite the impact face) of the specimen. A 3.19-mm-thick brass spacer was used for this shot. The gauge, spacer, and target assembly are then placed face down on a granite surface plate and aligned. Epoxy paste (Varian Torr-Seal) is placed around the periphery of the spacer to vacuum seal it to the gauge and specimen. Care is taken to ensure that no epoxy seeps into the regions between the spacer and gauge, and spacer and specimen. Epoxy paste is also used to seal the vacuum tube into the hole in the target assembly. Epoxy (Castall 300-RT 7) is then poured into the target cup to securely attach the capacitor gauge to the specimen. The tilt pin ends are positioned in the plane of the specimen to within 1 μm with an electronic height gauge and then secured. (Vacuum grease is initially placed on the threads of the tilt pins so they can be adjusted.) The target assembly is completed by attaching the tilt pins to electrical connectors (Microdot Part No. 031-0050-0001) that are located in the flange of the capacitor gauge. Figure 7 shows the completed capacitor gauge target assembly.

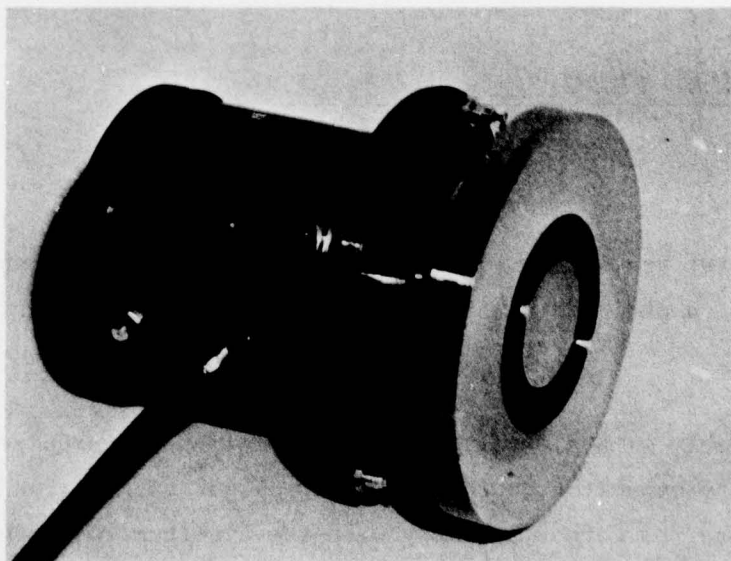


Figure 7. Completed target assembly with a capacitor gauge.

III. OPERATION OF CAPACITOR GAUGE

The results of the 6061-T6 aluminum symmetric impact experiment that was performed to check the operation of the capacitor gauge are presented in this section. Figure 8 shows the tilt pin data record and the capacitor gauge data record for this shot. The voltage-time pulse of the capacitor gauge record is converted to a free-surface velocity versus time profile using Equation (9) of the last section and known values for the equation parameters. For this shot the parameters are $R = 50.0 \Omega$, $E_0 = -3 \text{ kV}$, $A = 0.6390 \text{ pF mm}$, $B = 4.318 \text{ pF}$, $D = 0.047 \text{ mm}$, and $x_0 = 3.19 \text{ mm}$. Substituting these values into Equation (9) gives for the free-surface velocity

$$U_{fs} = \frac{0.103 \text{ V}}{\left[1 + 0.0328 \int_0^t V \text{ dt} \right]^2} \quad (10)$$

where V is the measured capacitor gauge voltage in mV, $\int_0^t V \text{ dt}$ is the area under the voltage-time pulse in mV μs , and U_{fs} is in mm/ μs or km/s. The free-surface position x can be obtained by substituting the above parameter values into Equation (8). The result is

$$x = 0.047 + \frac{3.143}{1 + 0.0328 \int_0^t V \text{ dt}} \quad (11)$$

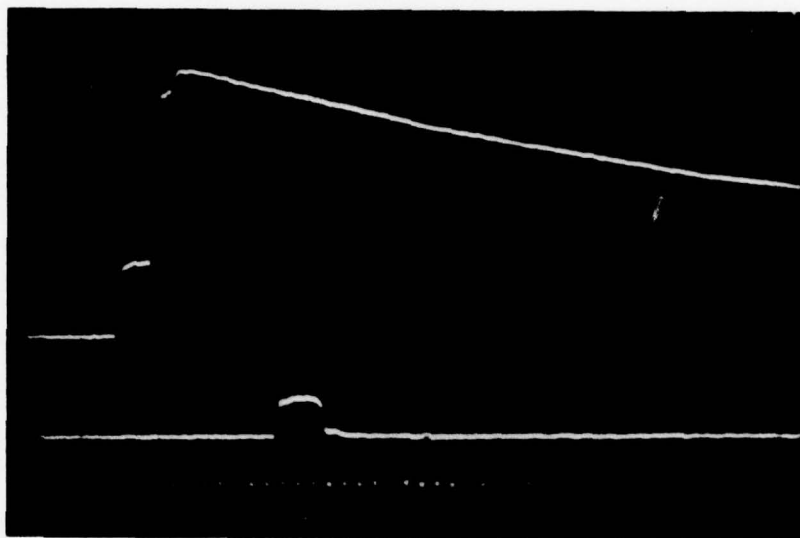
where x is in mm.

Two methods were used to obtain U_{fs} and x . In the first method a toolmaker's microscope was used to digitize the voltage-time pulse directly from the oscilloscope trace. The digitized data was used in the trapezoidal and Simpson's rules to obtain the area under the voltage-time pulse for selected times. Equation (10) was used to obtain the digitized free-surface-velocity profile. The x was obtained from Equation (11). Appendix C summarizes this procedure. In the second method an enlarged photograph was made from the capacitor gauge oscilloscope trace. The voltage-time pulse was digitized from this photograph. The area under the voltage-time pulse was obtained for selected times by cutting the photograph into pieces and weighing each piece. A standard-grid piece was weighed for calibration. This information is used in Equation (10) to

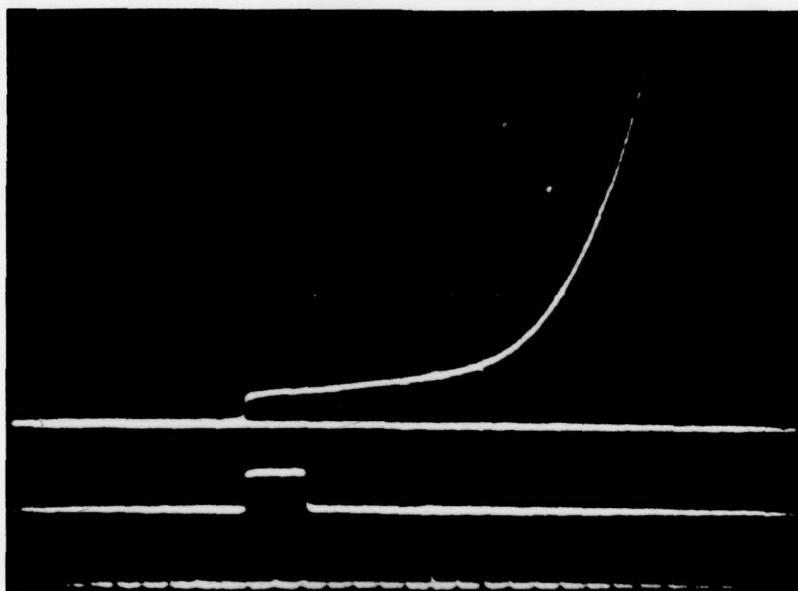
obtain the digitized free-surface velocity profile. Equation (11) was then used to obtain x . Table 2 gives the results of this computation. The results of both methods were in good agreement with each other. The read time for this capacitor gauge is estimated to be about 1 μ s. For times greater than this value, the free-surface velocity values begin to increase rapidly, probably due to relief wave effects originating from the edge of the specimen.⁶ Therefore Table 2 does not include any free-surface velocity values for times greater than 1 μ s. Equation (10) shows that when the term $0.0328 \int_0^t V dt \ll 1$, the free-surface velocity is proportional to V . For times less than 0.1 μ s, the free-surface velocity values in Table 2 are within about 1% of values obtained using only the term $0.103 V$ for U_{fs} .

Table 2. Digitized capacitor gauge voltage data and the corresponding free-surface-velocity and free-surface-position results for 6061-T6 aluminum.

Time (μ s)	Voltage V (mV)	Voltage-Time Integral $\int_0^t V dt$ (mV μ s)	Free-Surface Velocity U_{fs} (km/s)	Free-Surface Position x (mm)
0	0.79	0	0.081	3.19
0.077	1.14	0.07	0.116	3.18
0.089	6.98	0.13	0.714	3.18
0.106	7.35	0.24	0.746	3.17
0.206	8.00	0.99	0.774	3.09
0.310	8.73	1.81	0.802	3.01
0.413	9.53	2.71	0.829	2.93
0.514	10.26	3.69	0.842	2.85
0.612	11.13	4.77	0.858	2.76
0.715	12.15	5.94	0.877	2.68
0.816	13.24	7.18	0.894	2.59
0.916	14.55	8.59	0.913	2.50



(a)



(b)

Figure 8. Oscilloscope data from target assembly with a capacitor gauge. Time increases from left to right. (a) Tilt pin data record. The vertical scale is 4 V/div. The middle trace is an initial time reference square pulse for wave velocity measurements. A 0.01- μ s-period time calibration wave is shown at the bottom. (b) Capacitor gauge data record. The vertical scale is 20 mV/div. The middle trace is a 0.97- μ s delayed time reference square pulse for wave velocity measurements. A 0.10- μ s-period time calibration wave is shown at the bottom.

Figure 9 is a plot of the digitized free-surface-velocity data of Table 2. It shows a small amplitude elastic wave followed by a large amplitude plastic wave. The 0.081 km/s free-surface velocity for the elastic wave is somewhat larger than the value of 0.066 km/s obtained by Christman et al.⁷ using quartz gauges and a laser velocity interferometer. However, this agreement is reasonable considering that the elastic wave portion of the voltage pulse in Figure 8(b) has an amplitude only slightly above the zero level for the 20 mV/div vertical scale setting. The free-surface velocity for the plastic wave increases initially to a value of about 0.75 km/s and then increases at a slower rate to the 0.92 km/s measured impactor velocity.

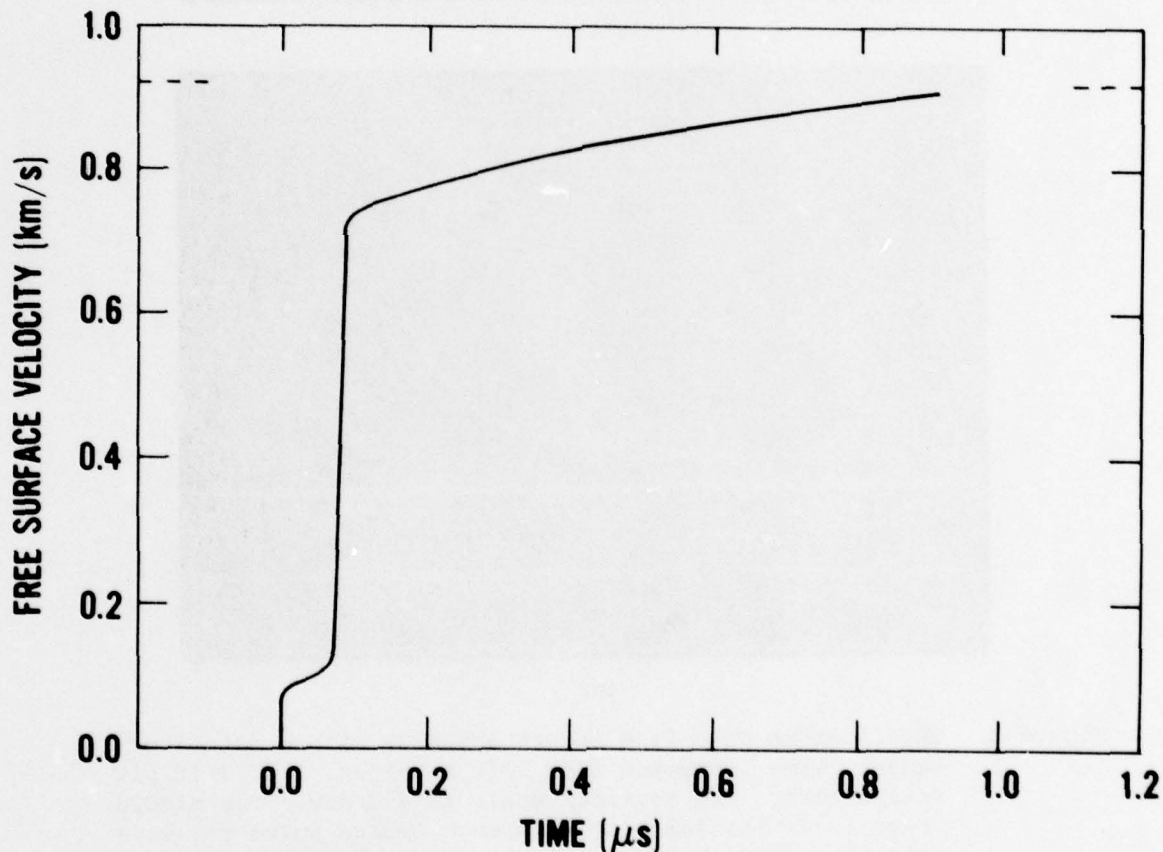


Figure 9. Free-surface velocity versus time profile for 6061-T6 aluminum. The horizontal dashed line is the 0.92 km/s measured impactor velocity.

Table 3 summarizes the shock wave results for the 6061-T6 aluminum symmetric impact experiment. The measured 6.44 km/s elastic wave velocity is in good agreement with the value of 6.40 km/s reported by Christman et al.⁷ The 0.70 GPa Hugoniot elastic limit is in reasonable agreement with the value of 0.57 GPa reported by Christman et al.⁷ The difference is probably due to the large previously mentioned measurement uncertainty for the elastic free-surface velocity. Christman et al.⁷ obtained $U_s = 5.24 + 1.40 u_p$ and $\sigma_H = 0.1 + 14.04 u_p + 3.77 u_p^2$ (U_s and u_p in km/s, and σ_H in GPa) for the shock velocity-particle velocity relationship and the stress-particle velocity relationship, respectively, for 6061-T6 aluminum for $\sigma_H \leq 20$ GPa. Shock velocity and stress values of 5.88 km/s and 7.36 GPa are calculated, respectively, using a 0.46 km/s plastic wave particle velocity in these equations. The measured shock velocity and stress values of 5.92 km/s and 7.40 GPa, respectively, are in good agreement with these calculated values.

Table 3. Summary of shock-wave results for 6061-T6 aluminum.

Shot No.	Description of Shot	Impactor Diameter (mm)	Impactor Thickness (mm)	Initial Impactor Density (Mg/m ³)	Specimen Diameter (mm)	Specimen Thickness (mm)	
160	6061-T6 Al + 6061-T6 Al/tilt pins, capacitor gauge	35.63	6.36	2.70	27.97	6.31	
Initial Specimen		Elastic Wave					
Shot No.	Projectile Density ρ_0 (Mg/m ³)	Projectile Velocity ^a U_0 (km/s)	Impactor Tilt (mrad)	Wave Velocity ^b U_e (km/s)	Particle Velocity ^c U_p (km/s)	Stress ^d σ_e (GPa)	Strain ^e $\Delta V/V_0$
160	2.70	0.919	0.63	6.44	0.041	0.70	0.0063
		Plastic Wave					
Shot No.	Wave Velocity ^b U_s (km/s)	Particle Velocity ^f U_p (km/s)	Stress ^g σ_H (GPa)	Strain ^h $\Delta V/V_0$			
160	5.92	0.46	7.40	0.077			

^a Average of two measurements. The estimated uncertainty is about 2%.

^b Calculated using the measured elastic and plastic wave transit times through the specimen disk. The plastic wave transit time was obtained using a half-amplitude value for the plastic wave free-surface velocity. The estimated wave velocity uncertainty is a few percent.

^c Taken as one-half the measured free-surface velocity of the elastic wave. The estimated uncertainty is about 10% due to the small measured value for the elastic wave free-surface velocity.

^d $\sigma_e = \rho_0 U_e U_p$.

^e $\Delta V_e/V_0 = 1 - V_e/V_0 = U_e/U_p$ where $V_0 = 1/\rho_0$.

^f $u_p = U_0/2$.

^g $\sigma_H = \sigma_e + \rho_e (U_s - U_e) (U_p - U_e)$ where $\rho_e/(1 - U_e/U_p)$.

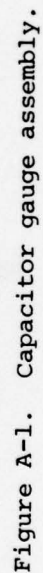
^h $\Delta V/V_0 = 1 - V/V_0$ where $V/V_0 = (1 - U_e/U_p) (U_s - U_p)/(U_s - U_e)$ and $V = 1/\rho$.

REFERENCES

1. W. Mock, Jr. and W. H. Holt, *The NSWC Gas Gun Facility for Shock Effects in Materials*, Naval Surface Weapons Center, Dahlgren Laboratory Technical Report NSWC/DL TR-3473, Dahlgren, VA, July 1976.
2. M. H. Rice, "Capacitor Technique for Measuring the Velocity of a Plane Conducting Surface," *The Review of Scientific Instruments*, Vol. 32, (1961), p. 409.
3. G. R. Fowles, "Experimental Technique and Instrumentation," *Dynamic Response of Materials to Intense Impulsive Loading*, Air Force Materials Laboratory, (1972), OH, p. 405.
4. S. Cochran and D. L. Banner, "Spall Studies in Uranium," *Journal of Applied Physics*, Vol. 48, (1977), p. 2729.
5. W. Mock, Jr. and W. H. Holt, "Device Used with Charged Pin Technique for Precision Gas Gun Projectile Velocity Measurements," *The Review of Scientific Instruments*, Vol. 45, (1974), p. 491.
6. D. L. Banner of Lawrence Livermore Laboratory observed a similar increase in the free-surface velocity using capacitor gauges. The increase was attributed to relief wave effects from the edge of the specimen. (private communication).
7. D. R. Christman, W. M. Isbell, S. G. Babcock, A. R. McMillan, and S. J. Green, *Measurements of Dynamic Properties of Materials*, Vol. III, 6061-T6 Aluminum, General Motors Technical Center Report DASA 2501-3, Warren, MI, November 1971.

APPENDIX A
ENGINEERING DRAWINGS FOR CAPACITOR GAUGE

(All dimensions in inches. To convert to
SI units use 1 in. = 25.4 mm.)



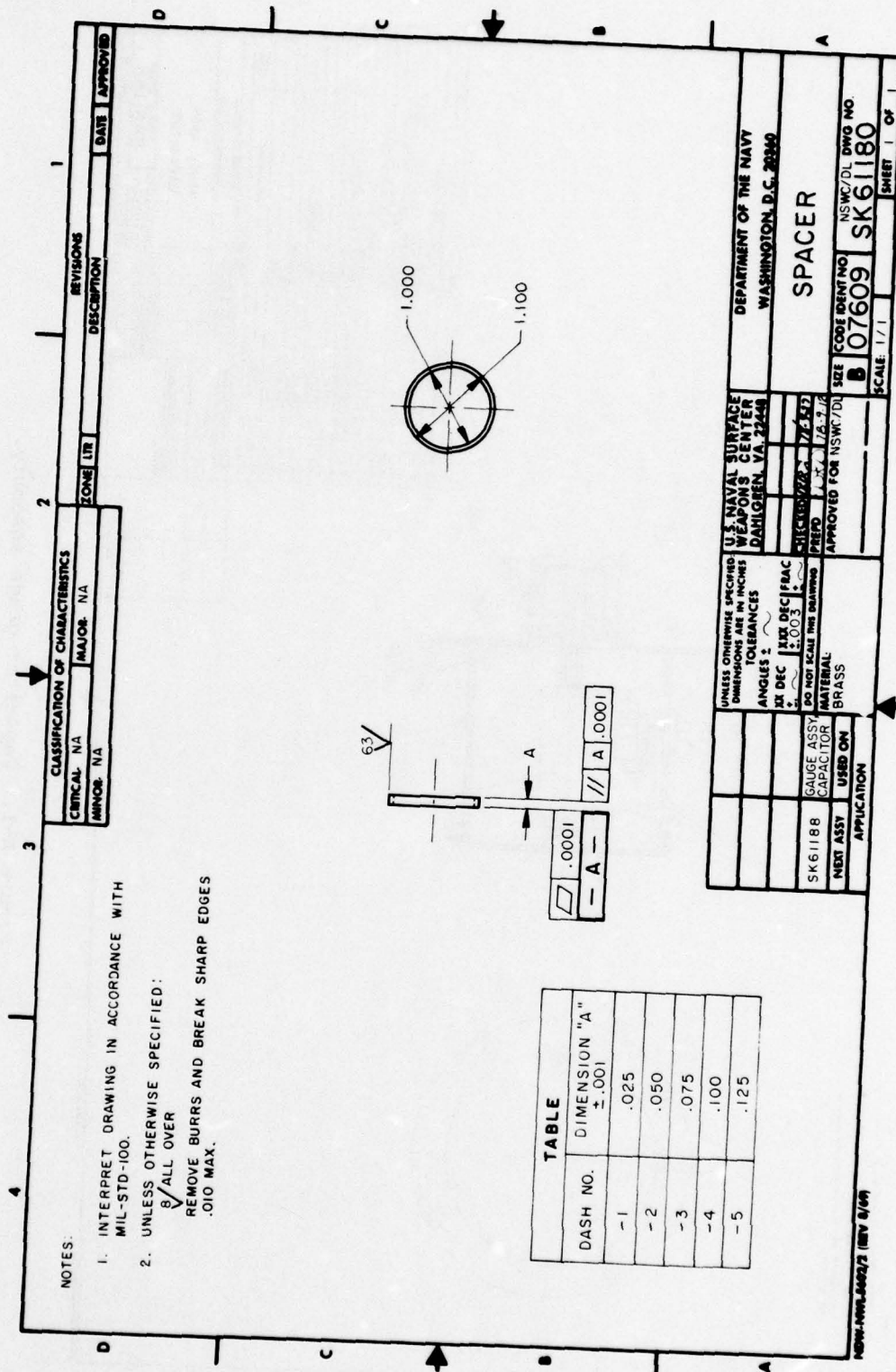


Figure A-2. Capacitor gauge spacer.

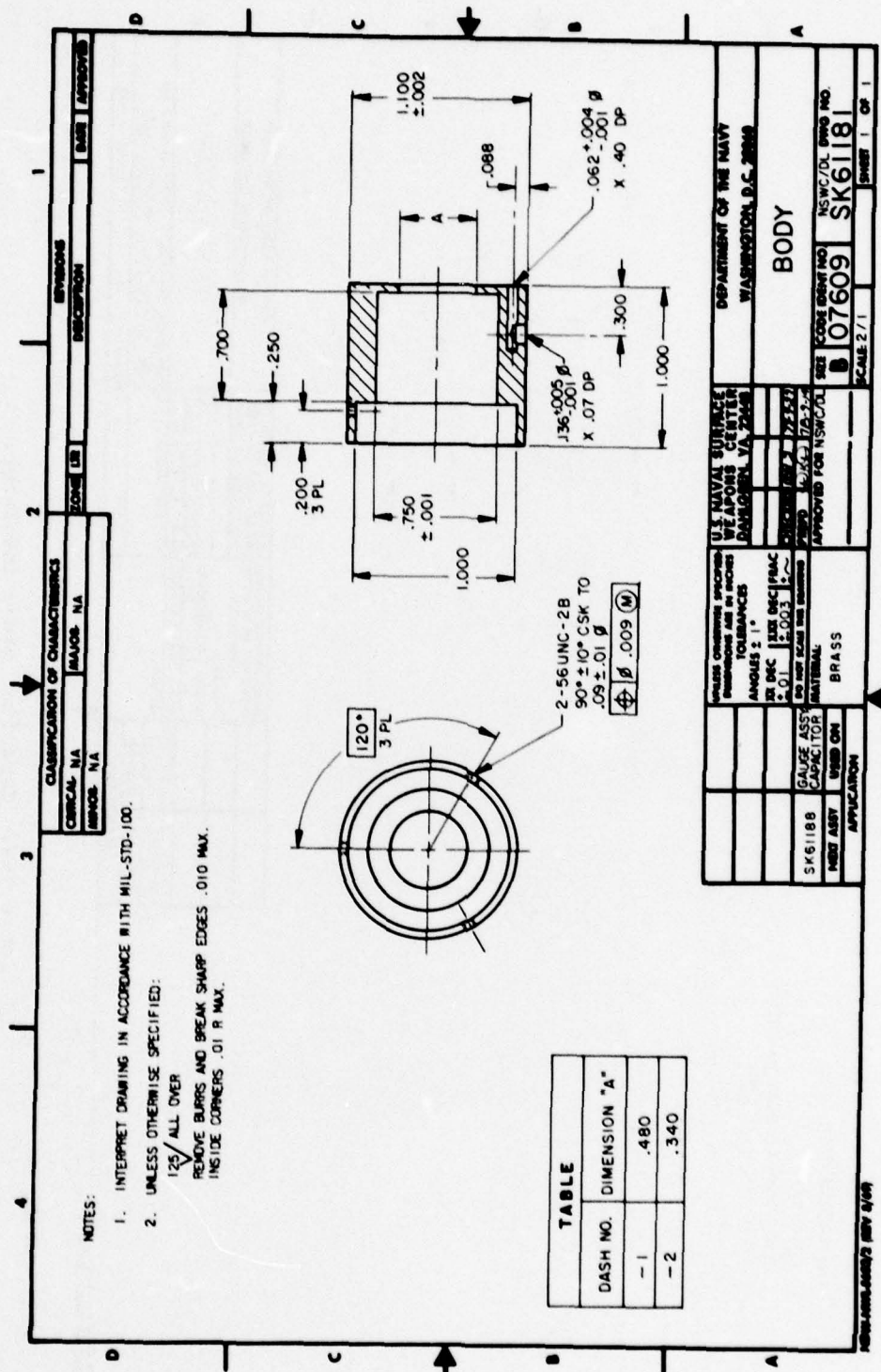


Figure A-3. Capacitor gauge body.

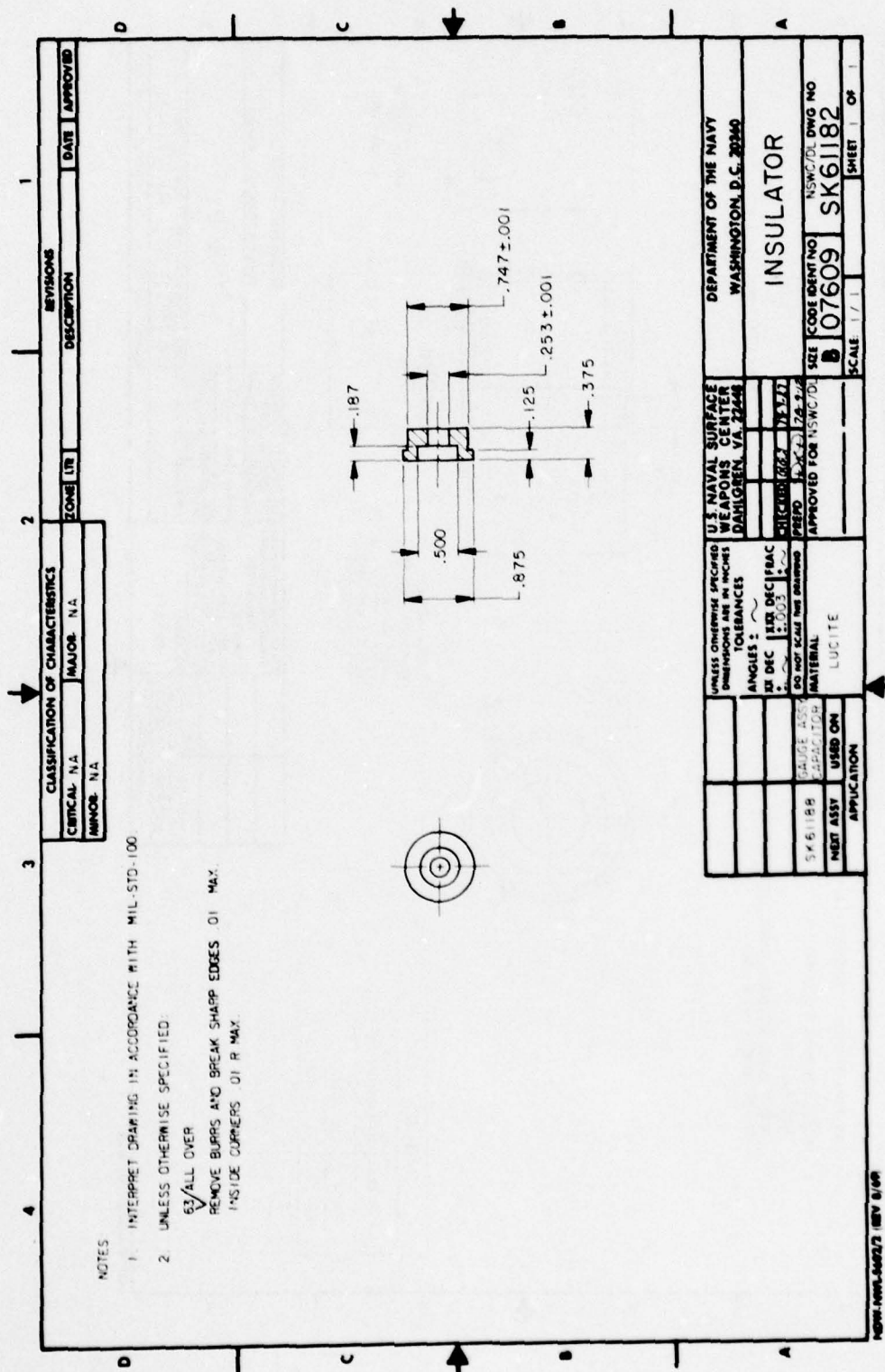


Figure A-4. Capacitor gauge insulator.

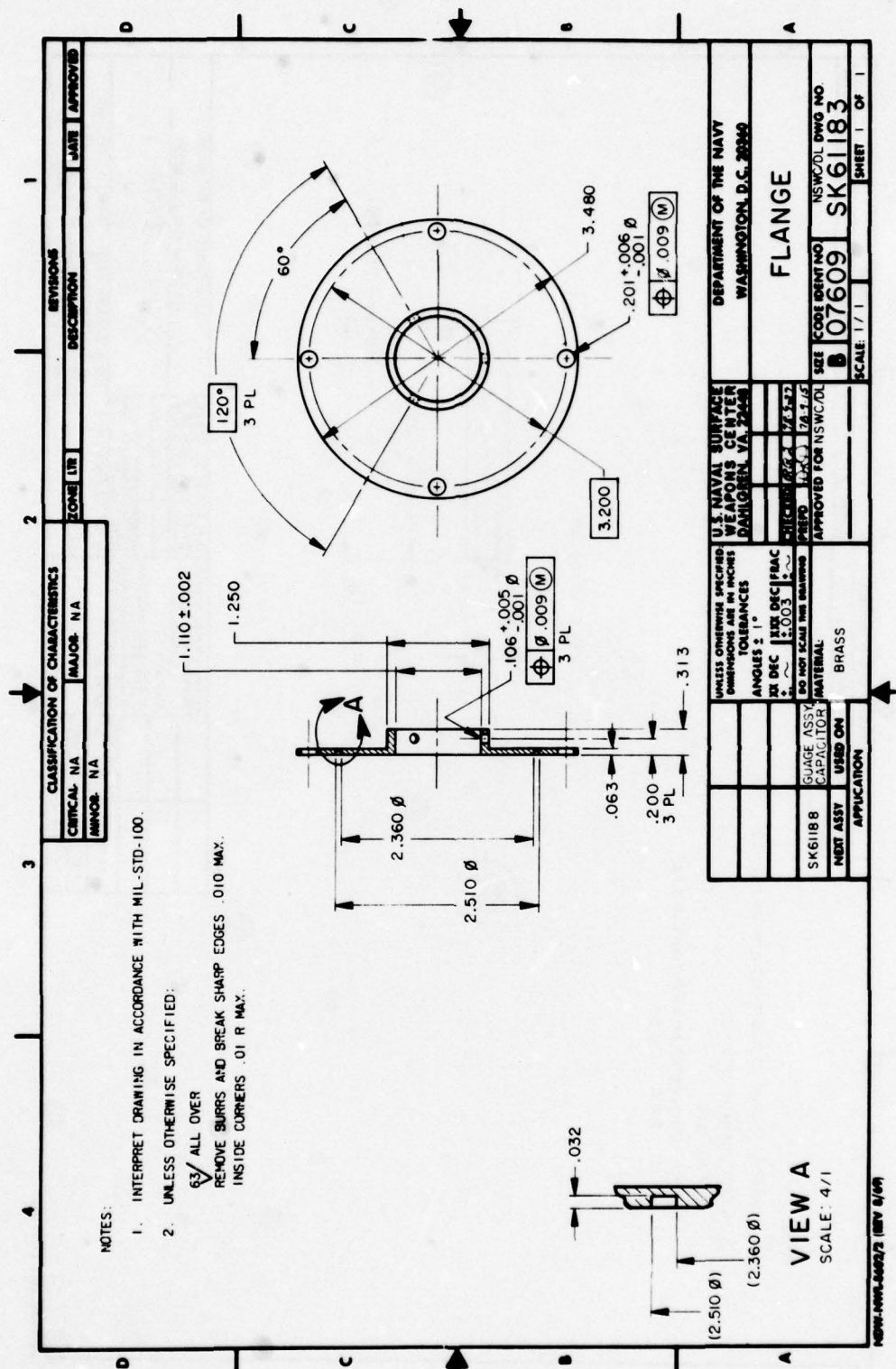


Figure A-5. Capacitor gauge flange.

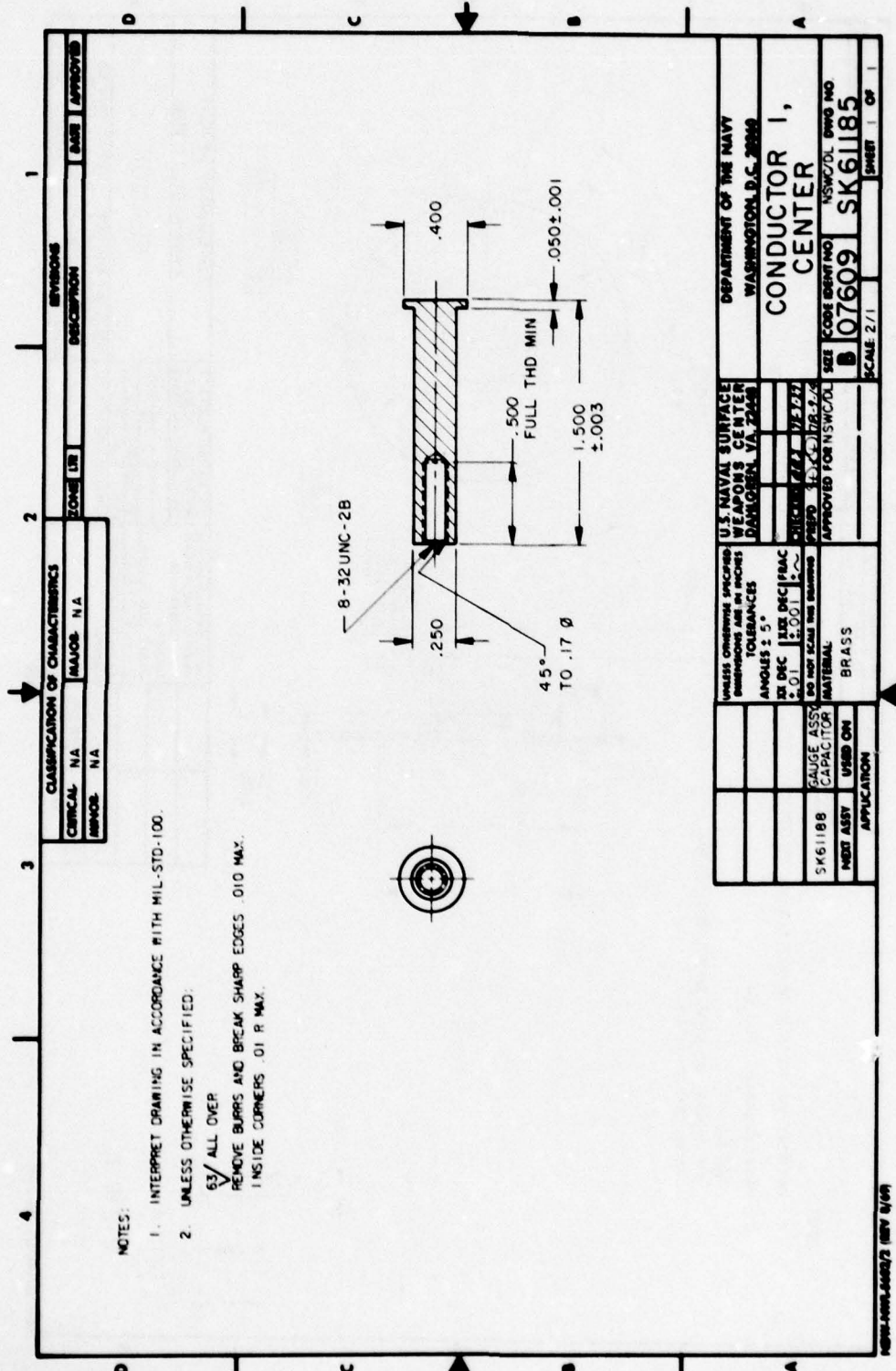


Figure A-6. Capacitor gauge center conductor 1.

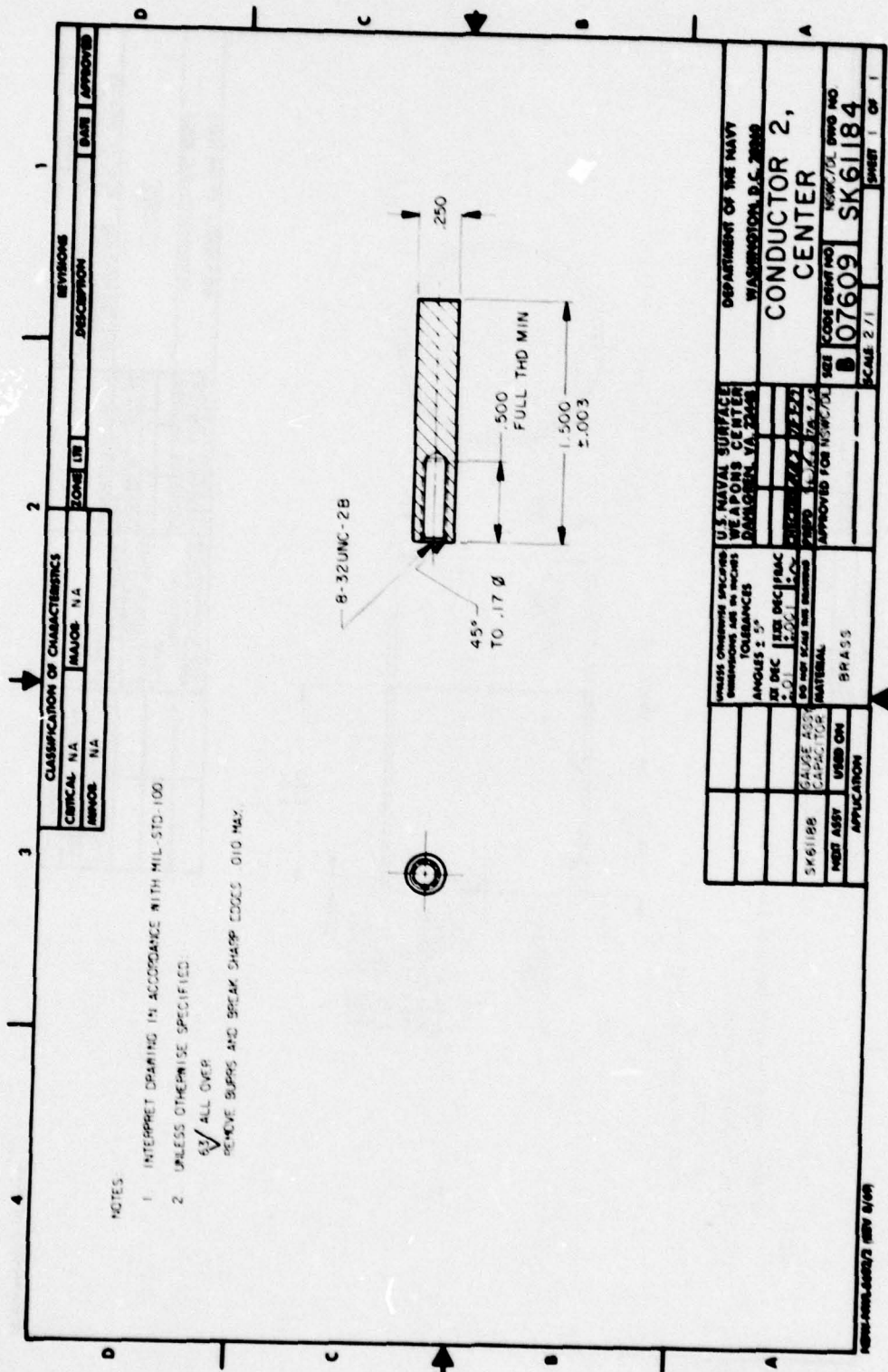


Figure A-7. Capacitor gauge center conductor 2.

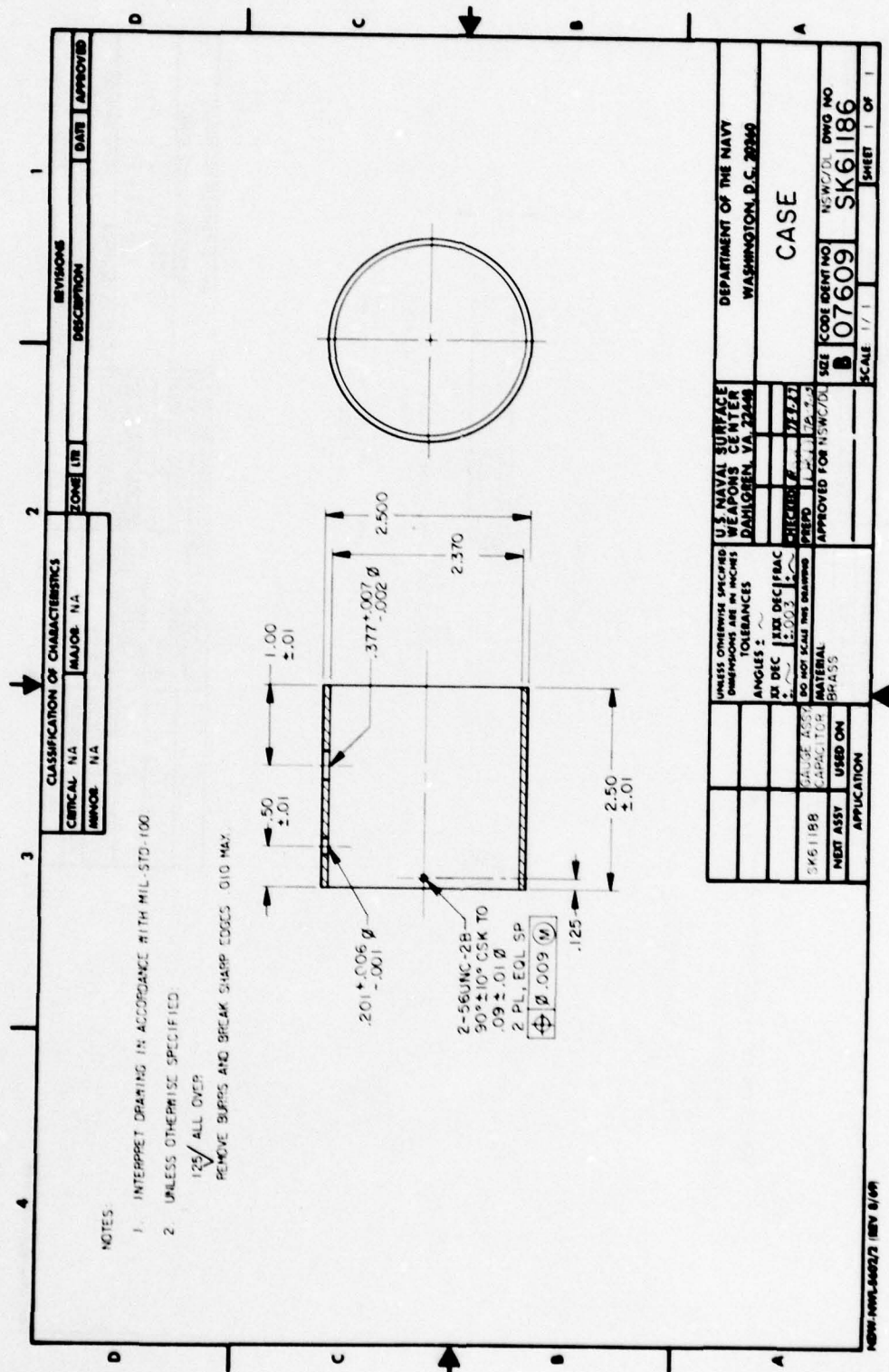


Figure A-8. Capacitor gauge case.

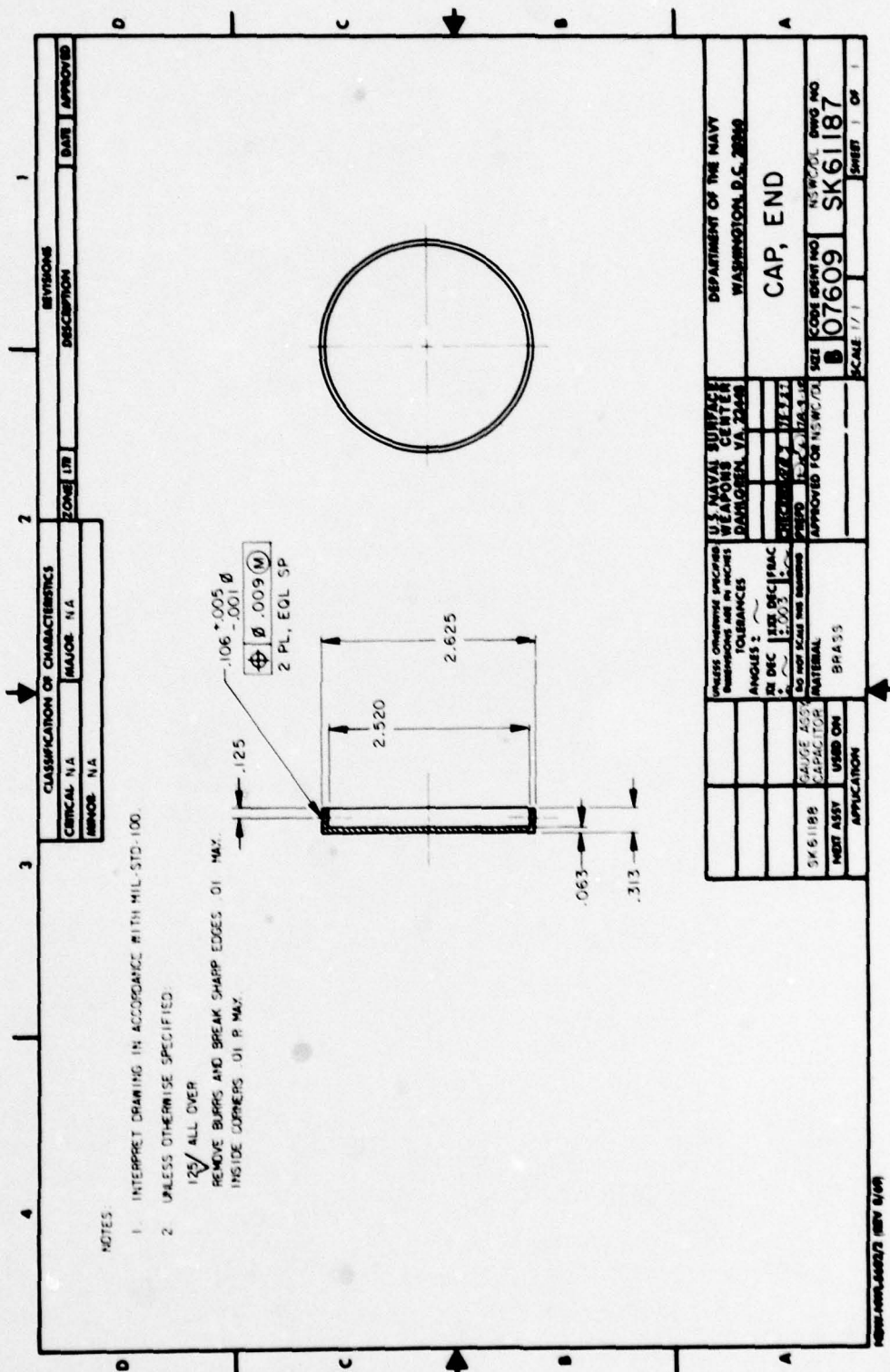


Figure A-9. Capacitor gauge end cap.

APPENDIX B
PLOTS FOR DETERMINING CAPACITOR GAUGE SPACER
THICKNESSES AND OSCILLOSCOPE SETTINGS
FOR VARIOUS FREE-SURFACE-VELOCITY VALUES

This section contains plots that can be used in estimating the capacitor gauge spacer thickness and oscilloscope settings for a gas gun experiment. For simplicity we will assume that the gauge capacitance is given by the equation

$$C = \frac{\epsilon_0 A_d}{x}, \quad (B-1)$$

where $\epsilon_0 = 8.854 \times 10^{-12} \text{ C N}^{-1} \text{ m}^{-2}$, A_d is the gauge disk area, and x is the spacing between the specimen and gauge disk. Equation (B-1) is simpler than Equation (1) which was used in the actual data analysis. Our capacitor gauge has been designed for disk diameters of 6.4 or 10.2 mm. Using these values in Equation (B-1) gives

$$C = \begin{cases} \frac{0.285}{x}, & \text{for 6.4-mm-diameter disk,} \\ \frac{0.723}{x}, & \text{for 10.2-mm-diameter disk,} \end{cases} \quad (B-2)$$

where C is in pF and x is in mm. The capacitor gauge voltage V can be obtained by substituting Equations (4) and (B-1) into Equation (5). The result is

$$V = - \frac{\epsilon_0 R E_0 A_d U_{fs}}{(x_0 - U_{fs} t)^2}. \quad (B-3)$$

Here we have assumed a constant free-surface velocity and used $x = x_0 - U_{fs} t$ where x_0 is the initial specimen spacing (spacer thickness). Letting $R_0 = 50 \Omega$, $E_0 = -3 \text{ kV}$, and using the two disk diameters gives

$$V = \begin{cases} \frac{42.7 U_{fs}}{(x_0 - U_{fs} t)^2}, & \text{for 6.4-mm-diameter disk,} \\ \frac{109 U_{fs}}{(x_0 - U_{fs} t)^2}, & \text{for 10.2-mm-diameter disk,} \end{cases} \quad (B-4)$$

where V is in mV, U_{fs} in mm/ μ s or km/s, x_0 is in mm, and t is in μ s. Equation (B-4) was used to obtain Figures B-1, B-2, and B-3. The calculated voltage-time profiles can be used for selecting a spacer thickness and disk diameter for an expected free-surface-velocity value in a gas gun experiment. The free-surface-velocity range was chosen to be similar to the 0.03 to 1 km/s projectile velocity range for our gas gun. The time axis was chosen to be about twice the measured 0.9- μ s read time for the capacitor gauge. A spacer thickness and disk diameter that gives a voltage-time profile with an initial voltage greater than 10 to 15 mV and that is slowly rising for about 1 μ s should be appropriate for a free-surface-velocity measurement. The initial capacitor gauge voltage versus free-surface velocity is shown in more detail in Figures B-4 and B-5. These figures were generated using Equation (B-3) with $t = 0$ and selected values for the spacer thickness x_0 .

Figure B-6 is a plot of the time for the capacitor gauge voltage to increase a certain amount versus the specimen free-surface velocity. Voltage ratios V_F/V_0 of 4, 8, and 12 were chosen since they correspond to reasonable dynamic ranges for setting the oscilloscope vertical. The curves in Figure B-6 were obtained from the equation

$$t_F = \frac{x_0}{U_{fs}} \left[1 - \left(\frac{V_F}{V_0} \right)^{-1/2} \right] \quad , \quad (B-5)$$

where t_F is the time corresponding to a capacitor gauge voltage V_F . Equation (B-5) was obtained using Equation (B-3) to determine the voltages V_0 and V_F and then forming the ratio V_F/V_0 .

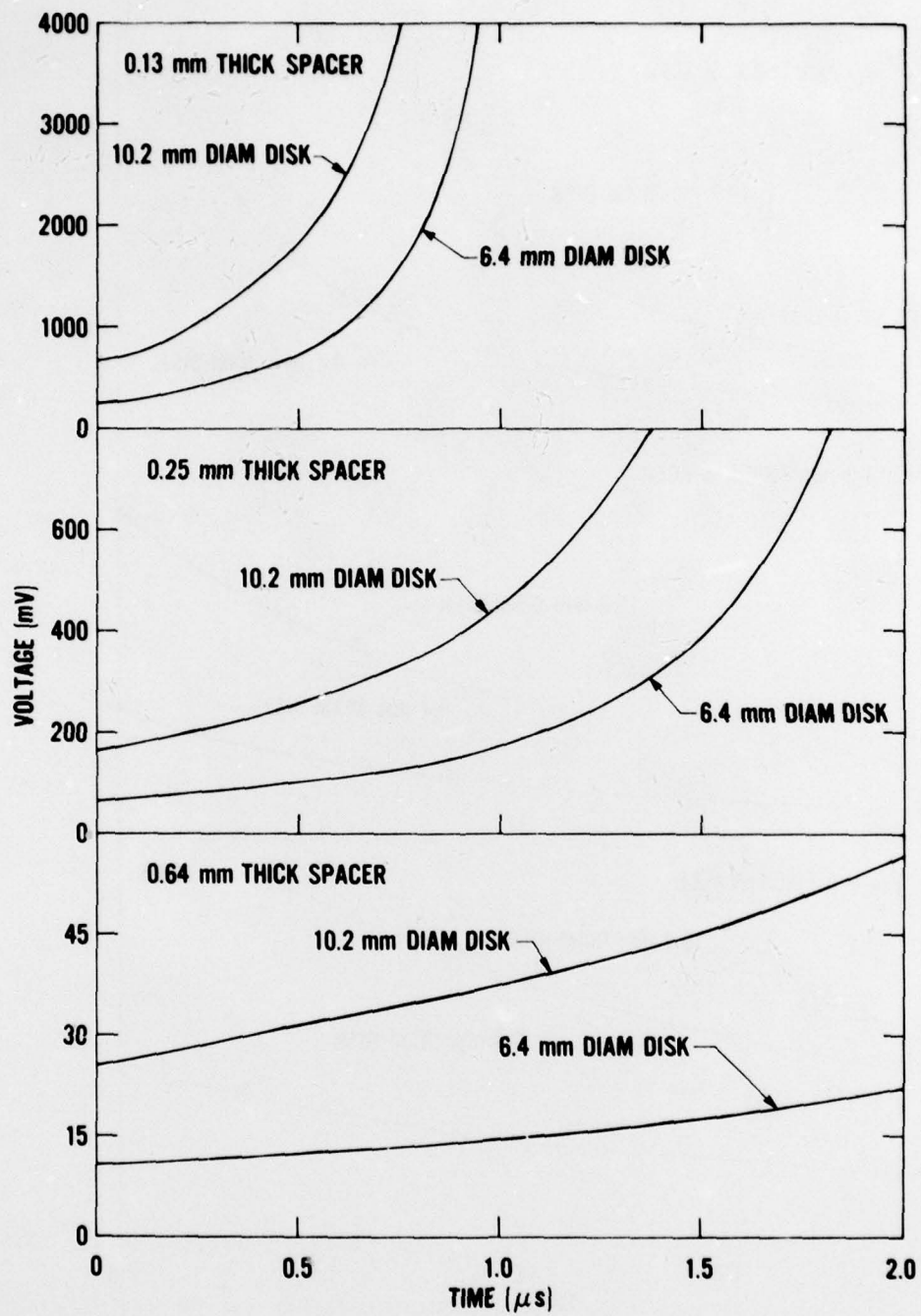


Figure B-1. Capacitor gauge voltage-time profiles for 6.4- and 10.2-mm-diameter gauge disks and selected spacer thicknesses at a constant specimen free-surface velocity of 0.1 km/s.

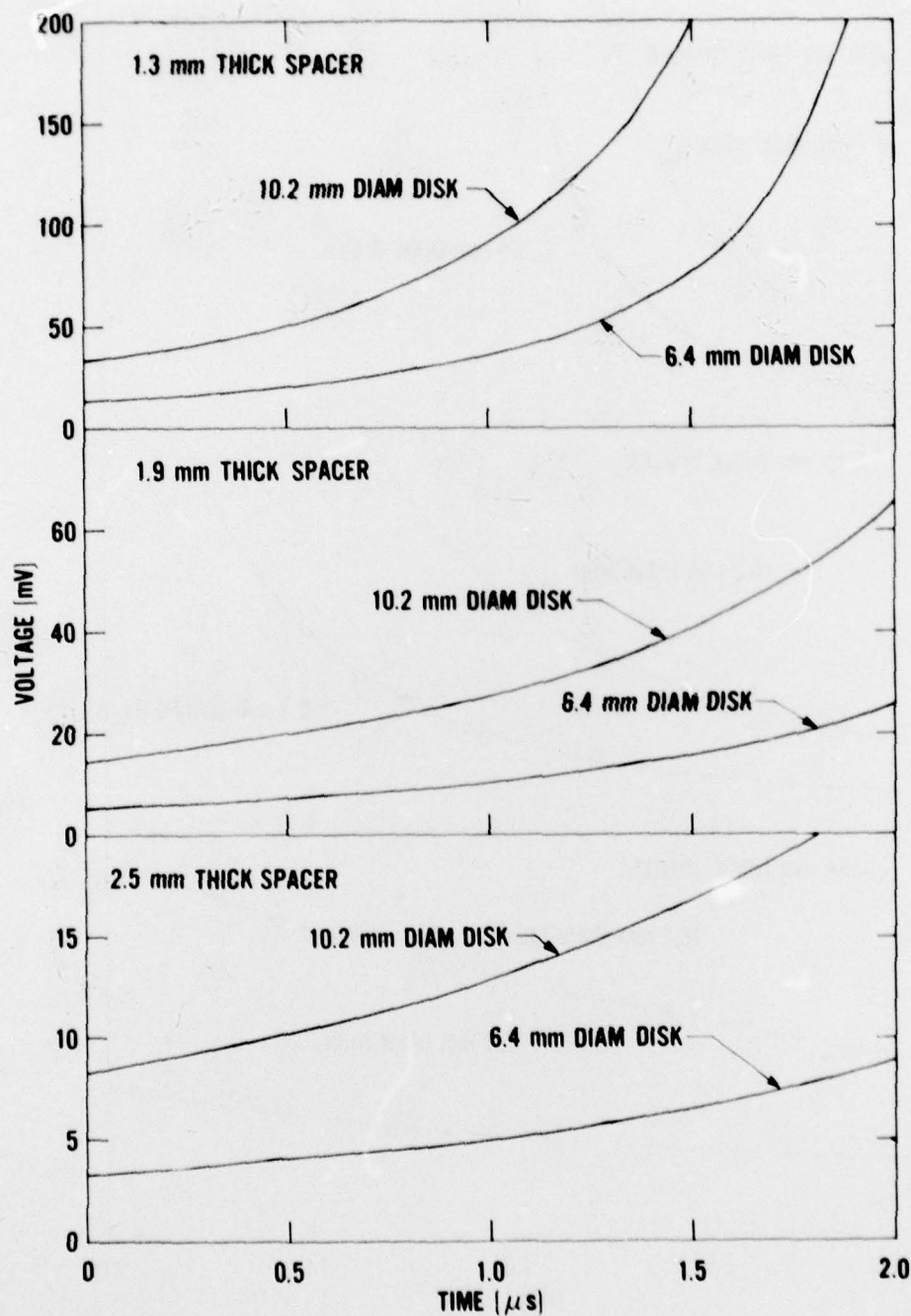


Figure B-2. Capacitor gauge voltage-time profiles for 6.4- and 10.2-mm-diameter gauge disks and selected spacer thicknesses at a constant specimen free-surface velocity of 0.5 km/s.

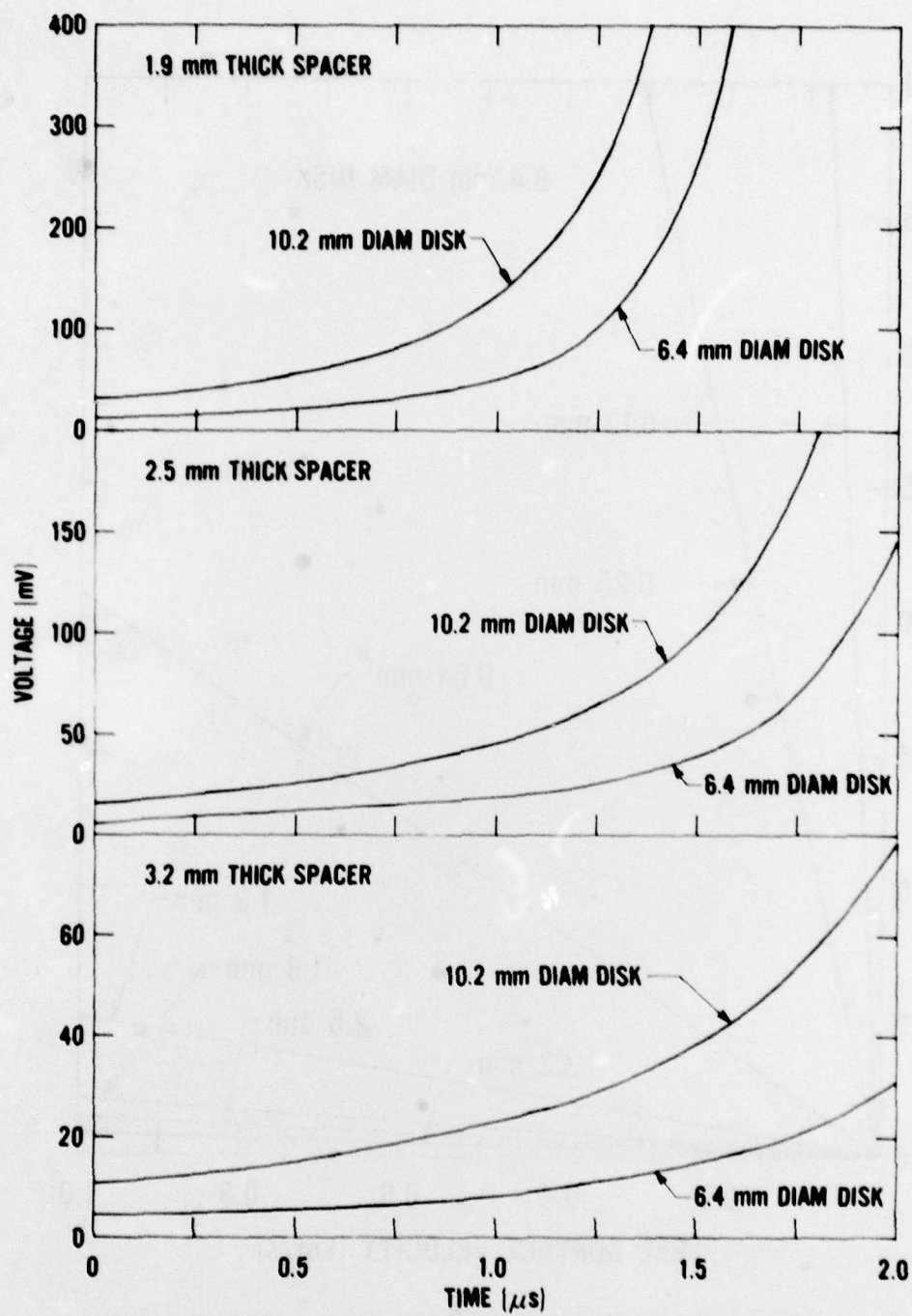


Figure B-3. Capacitor gauge voltage-time profiles for 6.4- and 10.2-mm-diameter gauge disks and selected spacer thicknesses at a constant specimen free-surface velocity of 1 km/s.

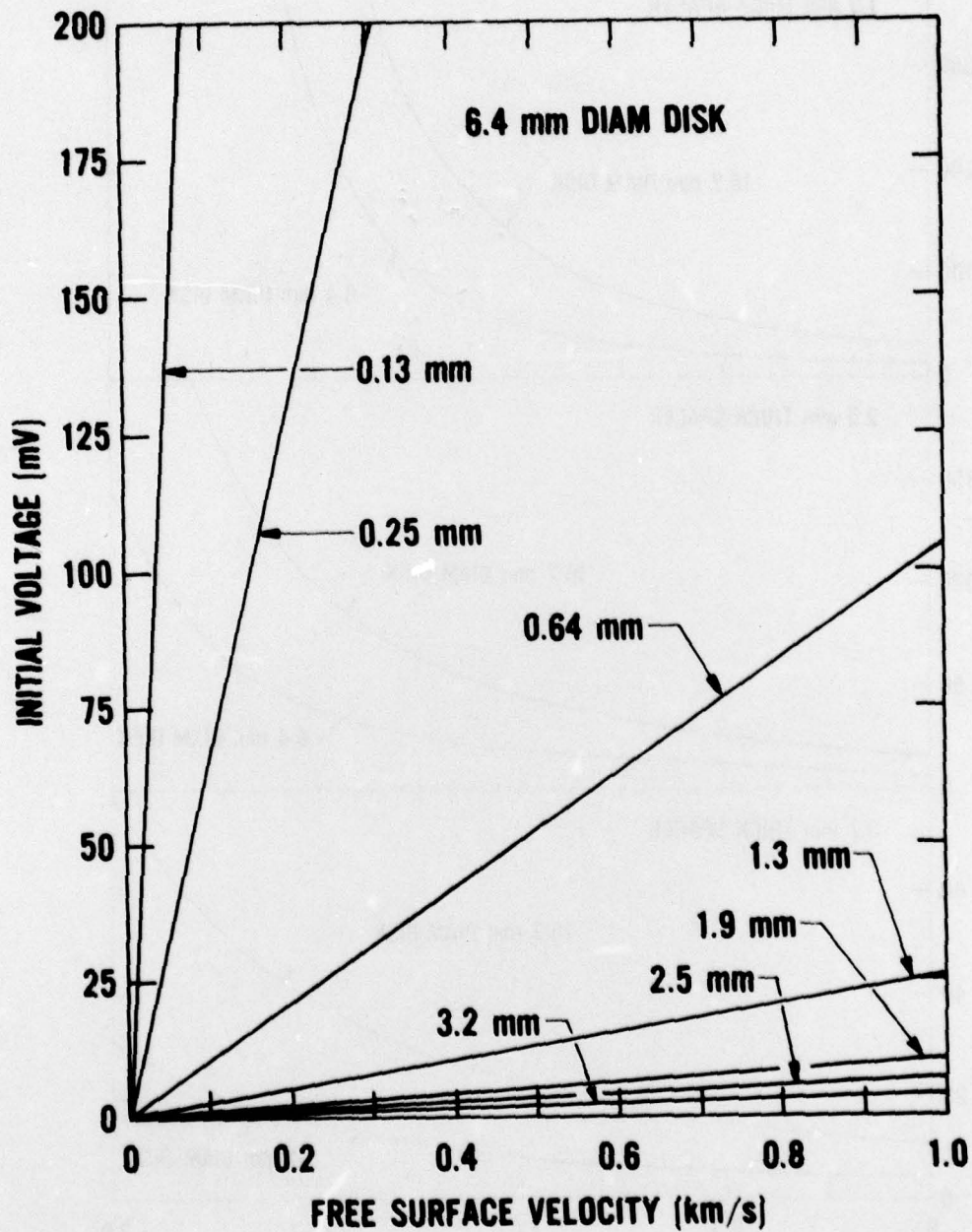


Figure B-4. Initial capacitor gauge voltage versus specimen free-surface-velocity curves for selected spacer thicknesses for a 6.4-mm-diameter gauge disk. Each curve is labeled with the corresponding spacer thickness.

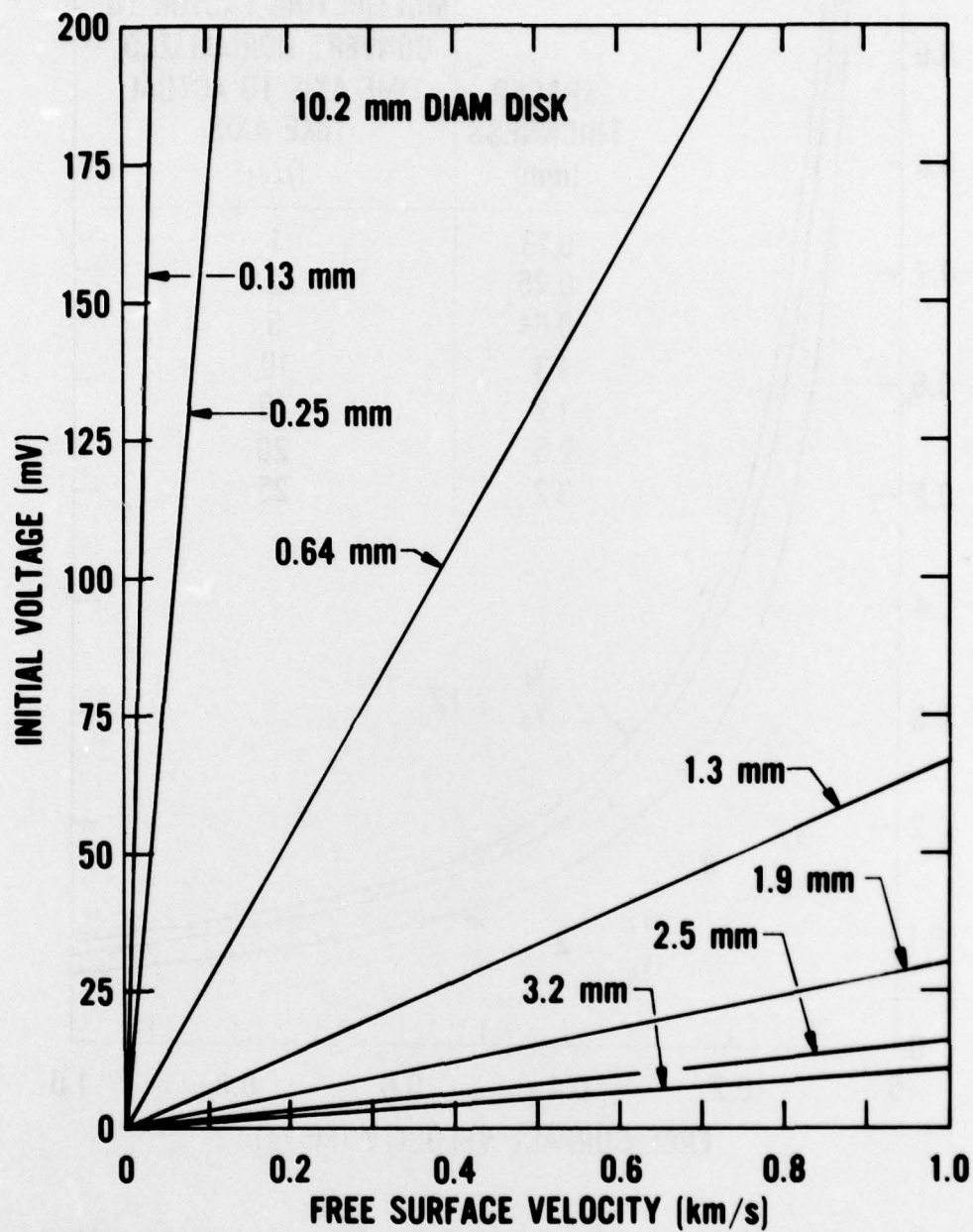


Figure B-5. Initial capacitor gauge voltage versus specimen free-surface-velocity curves for selected spacer thicknesses for a 10.2-mm-diameter gauge disk. Each curve is labeled with the corresponding spacer thickness.

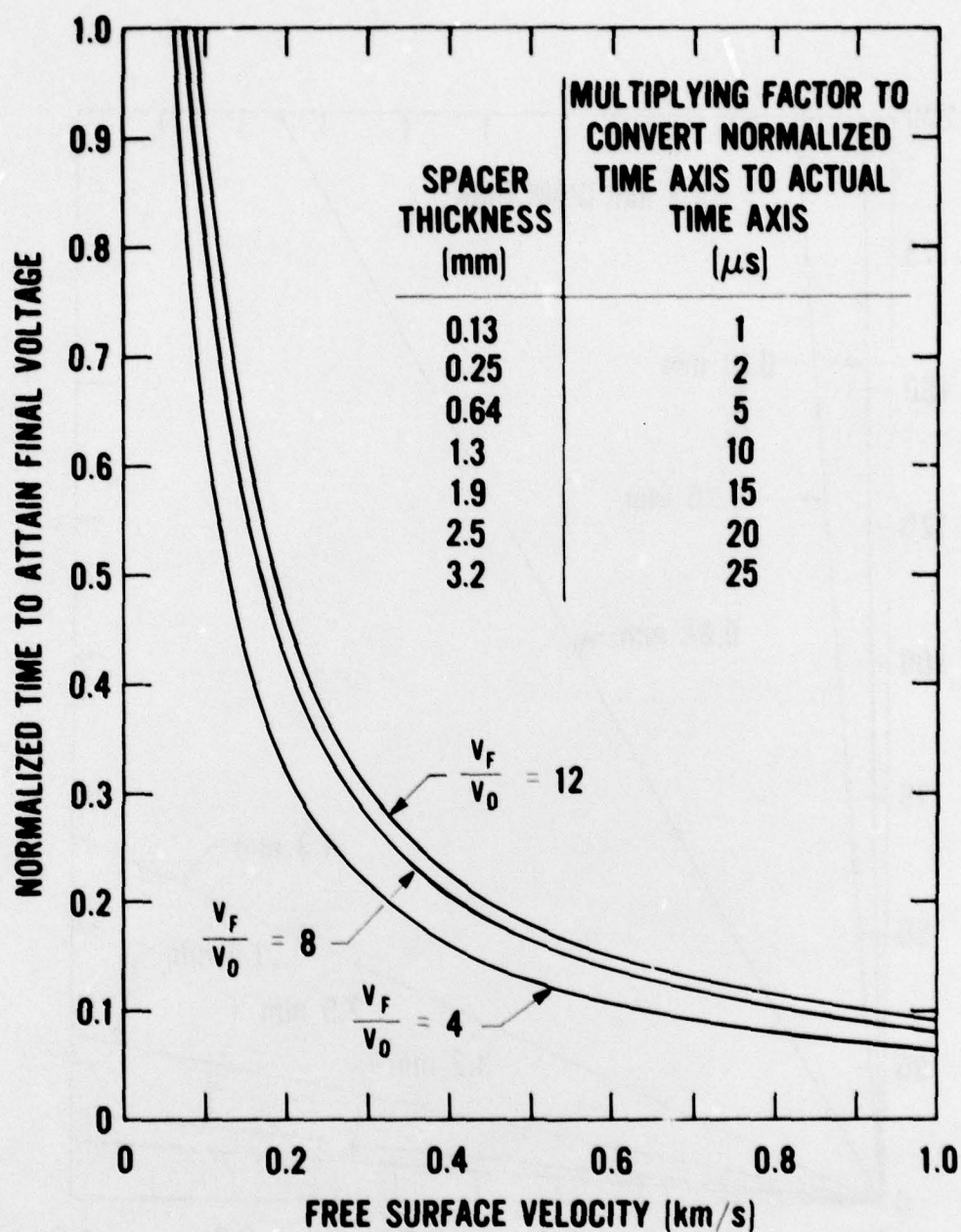


Figure B-6. Normalized time to attain final capacitor gauge voltage versus specimen free-surface velocity for selected spacer thicknesses. Curves are given for $V_F/V_0 = 4, 8$, and 12 where V_0 and V_F are the initial and final capacitor gauge voltage values, respectively. The time axis for a selected spacer thickness can be determined by multiplying the normalized time axis by the appropriate factor given in the figure.

APPENDIX C

INTEGRATION OF CAPACITOR GAUGE VOLTAGE PULSE

USING THE TRAPEZOIDAL AND SIMPSON'S RULES

It was stated in Section III that the trapezoidal and Simpson's rules were used to obtain the area under the capacitor gauge voltage-time pulse. The results are presented in this appendix. Table C-1 contains the free-surface velocity and the free-surface position calculations. Figure C-1 is a plot of the digitized free-surface velocity points. The trapezoidal rule was used for the initial fast-rising portion of the voltage pulse since that part of the pulse could be easily subdivided into linear sections at points of slope discontinuities. The first four nonzero voltage-time integral values in Table C-1 were obtained with the trapezoidal rule. The rule for obtaining the area of a segment $A_{i-1,i}$ for the time interval $(t_i - t_{i-1})$ is

$$A_{i-1,i} = \frac{1}{2} (V_{i-1} + V_i) (t_i - t_{i-1}) , \quad (C-1)$$

where $i = 1, 2, 3$, etc., and V_i is the digitized voltage at time t_i . Here $t_0 = 0$. For our case, the area segments $A_{0,1}$, $A_{1,2}$, $A_{2,3}$, and $A_{3,4}$ were obtained for $i = 1, 2, 3$, and 4 , respectively. The remaining segments were obtained using Simpson's rule. This rule states that the area segment $A_{i-2,i}$ for two adjacent and equal time intervals $(t_{i-1} - t_{i-2})$ and $(t_i - t_{i-1})$ is given by

$$A_{i-2,i} = \frac{1}{3} (V_{i-2} + 4V_{i-1} + V_i) (t_i - t_{i-1}) , \quad (C-2)$$

where $i = 2, 4, 6$, etc. For our case, the 13 area segments $A_{4,6}$, $A_{6,8}$, ..., $A_{28,30}$ were obtained for $i = 6, 8, \dots, 30$, respectively.

Table C-1. Free-surface-velocity and free-surface-position results using the trapezoidal and Simpson's rules for integrating the capacitor gauge voltage pulse.

Time ^a (μ s)	Voltage ^a V (mV)	Voltage-Time Integral ^b $\int_0^t V dt$ (mV μ s)	Free-Surface Velocity ^c U _{fs} (km/s)	Free-Surface Position ^c x (mm)
0	0.79	0	0.081	3.19
0.077	1.14	0.07	0.116	3.18
0.094	6.82	0.14	0.696	3.18
0.128	7.39	0.38	0.743	3.15
0.158	7.72	0.61	0.765	3.13
0.188	8.02	-	-	-
0.218	8.17	1.09	0.786	3.08
0.248	8.31	-	-	-
0.278	8.48	1.59	0.790	3.03
0.308	8.61	-	-	-
0.338	8.91	2.10	0.804	2.99
0.367	8.97	-	-	-
0.397	9.14	2.64	0.798	2.94
0.427	9.41	-	-	-
0.457	9.68	3.21	0.817	2.89
0.487	9.83	-	-	-
0.517	10.11	3.80	0.825	2.84
0.547	10.41	-	-	-
0.577	10.62	4.42	0.836	2.79
0.607	10.87	-	-	-
0.637	11.09	5.07	0.841	2.74
0.667	11.46	-	-	-
0.697	11.64	5.75	0.849	2.69
0.726	12.09	-	-	-
0.757	12.33	6.48	0.865	2.64
0.787	12.70	-	-	-
0.817	13.09	7.24	0.882	2.59
0.847	13.32	-	-	-
0.877	13.78	8.04	0.890	2.53
0.907	14.29	-	-	-
0.937	14.79	8.89	0.914	2.48

^aThese values were obtained directly from the capacitor gauge voltage-time oscilloscope trace using a toolmaker's microscope.

^bThe trapezoidal rule was used to obtain the first four nonzero values in this column. Simpson's rule was used to obtain the remaining non-zero values.

^cThe free-surface-velocity and free-surface-position values were obtained using Equations (10) and (11), respectively.

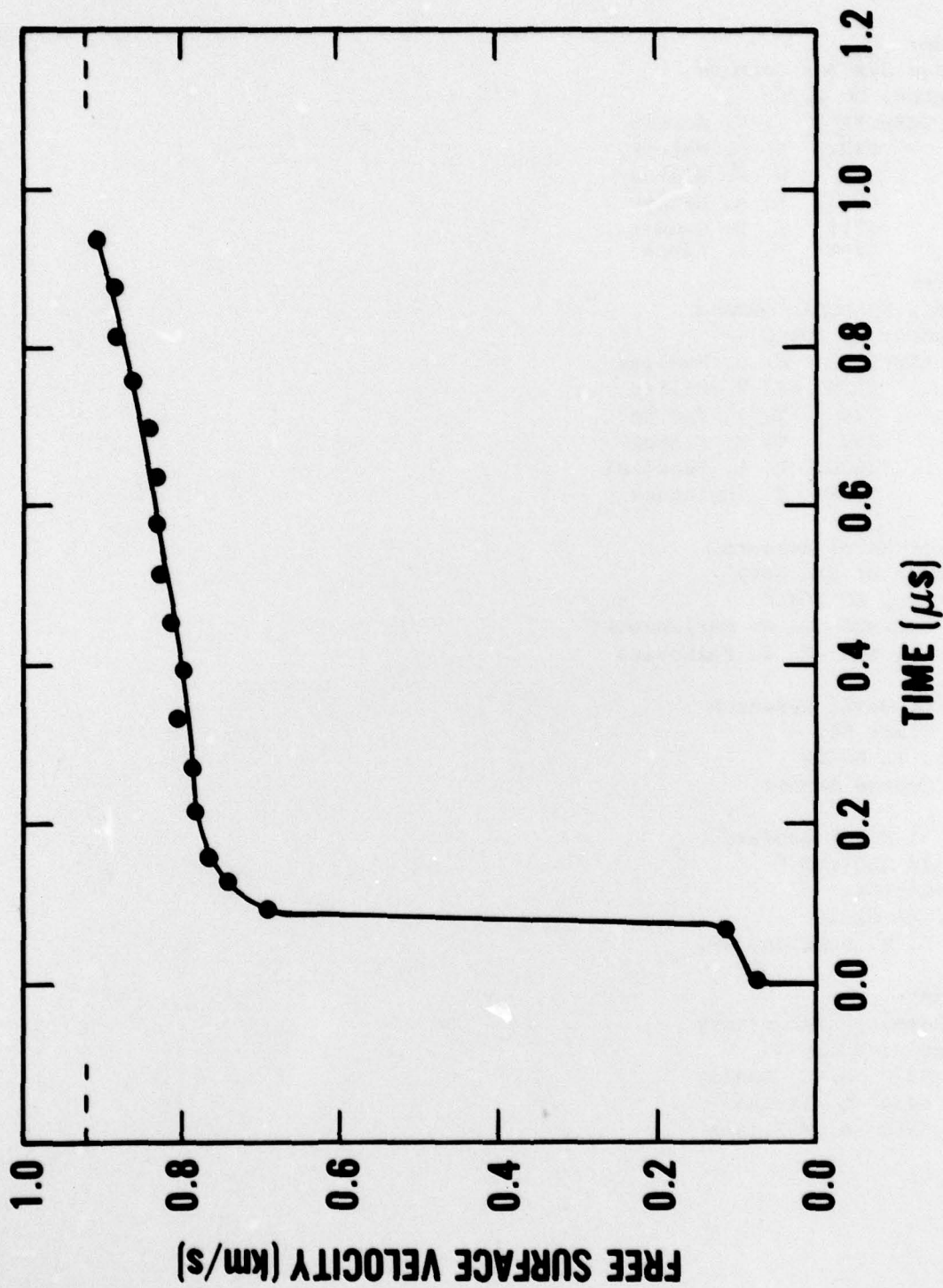


Figure C-1. Free-surface velocity versus time profile for 6061-T6 aluminum using the trapezoidal and Simpson's rules for integration of the capacitor gauge voltage-time pulse. The horizontal dashed line is the 0.92 km/s measured impactor velocity.

DISTRIBUTION

Commander
Naval Sea Systems Command
Washington, DC 20360
ATTN: SEA-05R G. N. Sorkin
05R22 S. J. Matesky
62R W. W. Blaine
62R31 R. A. Bailey
621Y L. H. Hawver
624R M. A. Kinna

Commander
Naval Air Systems Command
Washington, DC 20360
ATTN: AIR-310 H. J. Mueller
310B J. W. Willis
320 T. F. Kearns
350 E. M. Fisher
350D H. B. Benefiel
5324C S. Englander

Office of Naval Research
Department of the Navy
Washington, DC 20360
ATTN: ONR-420 T. G. Berlincourt
465 E. I. Salkovitz

Office of Naval Research
536 S. Clark St.
Chicago, IL 60605
ATTN: George Sandoz

Office of Naval Research
Bldg. 114 Section D
666 Summer St.
Boston, MA 02210
ATTN: L. H. Peebles, Jr.

Commander
Naval Research Laboratory
Washington, DC 20375
ATTN: 6370 S. C. Sanday
6434 E. Skelton
7908 A. Williams

Commander
Naval Weapons Center
China Lake, CA 93555
ATTN: M. E. Backman
R. L. Ballenger
J. Pearson
T. Zulkowski

Director
Army Ballistics Research Laboratories
Terminal Ballistics Laboratory
Aberdeen Proving Ground, MD 20015
ATTN: W. S. deRosset
W. Gillich
G. E. Hauver
G. Moss
R. Vitali

Commander
Army Materials and Mechanics Research Center
Watertown, MA 02172
ATTN: D. T. Dandekar
R. M. Lamothe
J. F. Mescall

Commander
Army Research and Development Command
Dover, NJ 07801
ATTN: C. deFranco
F. J. Owens

Commander
Army Waterways Experiment Station
Vicksburg, MS 39180
ATTN: D. R. Coltharp

Los Alamos Scientific Laboratory
Los Alamos, NM 87544
ATTN: J. J. Dick
J. M. Holt, Jr.
R. Morales
J. A. Morgan
Technical Library

(2)

Sandia Laboratories
Albuquerque, NM 87115
ATTN: R. A. Graham

Lawrence Livermore Laboratory
University of California
Livermore, CA 94550
ATTN: D. L. Banner
S. Cochran
A. Romero

Shock Dynamics Laboratory
Washington State University
Pullman, WA 99163
ATTN: G. E. Duvall
G. R. Fowles

Stanford Research Institute
Poulter Laboratory
333 Ravenswood Avenue
Menlo Park, CA 94025
ATTN: D. Curran
L. Seaman
D. Shockey

Defense Documentation Center
Cameron Station
Alexandria, VA 22314 (12)

Library of Congress
Washington, DC 20540
ATTN: Gift and Exchange Division (4)

Local:

C	
D	
E41	
F	
F10	
F12 (Berger)	
G	
G05	
G10	
G10 (Williams)	
G13	
G20	
G22	
G22 (Shuler)	G50
G30	G60
G301	R
G31	R04
G32	R10
G33	R12 (Erkman)
G34	R13
G34 (Hales)	R13 (Forbes)
G35	R13 (Roslund)
G35 (Mock)	R30
G35 (Holt)	X210
G35 (Wishard)	X2101 (GIDEP) (2)
G40	X211